GL-TR-89-0326

Measurements of the High Altitude Infrared Characteristics of the Atmosphere

F. H. Murcray
F. J. Murcray
R. D. Blatherwick
A. Goldman
D. G. Murcray

University of Denver
Department of Physics
Denver, CO 80208

October 1989

Final Report
6 June 1986 - 30 September 1989

GEOPHYSICS LABORATORY
AIR FORCE SYSTEMS COMMAND
UNITED STATES AIR FORCE
HANSCOM AIR FORCE BASE, MASSACHUSETTS 01731-5000

This technical report has been reviewed and is approved for publication

(Signature)
Michael Hoke
Contract Monitor

(Signature)
George A. Vanasse
Branch Chief

FOR THE COMMANDER

(Signature)
R. Earl Good
Division Director

This report has been reviewed by the ESD Public Affairs Office(PA) and is releasable to the National Information Service (NTIS).

Qualified requestors may obtain additional copies from the Defense Technical Information Center. All others should apply to the National Technical Information Service.

If your address has changed, or if you wish to be removed from the mailing list, or if the addressee is no longer employed by your organization, please notify GL/IMA, Hanscom AFB, MA 01731. This will assist us in maintaining a current mailing list.

Do not return copies of this report unless contractual obligations or notices on a specific document requires that it be returned.

REPORT DOCUMENTATION PAGE

Form Approved
OMB No. 0704-0188

1. AGENCY USE ONLY (Leave blank)	2. REPORT DATE	3. REPORT TYPE AND DATES COVERED
	October 1989	Final Report 6 June 1986-30 September 1989

4. TITLE AND SUBTITLE
Measurements of the High Altitude Infrared Characteristics of the Atmosphere

5. FUNDING NUMBERS
PE 61102F
P2310G1BL
Contract F19628-86-K-0029

6. AUTHOR(S)
F.H. Murcray, F.J. Murcray, D.G. Murcray, A. Goldman and R.D. Blatherwick

7. PERFORMING ORGANIZATION NAME(S) AND ADDRESS(ES)
University of Denver
Department of Physics
Denver, CO 80208

8. PERFORMING ORGANIZATION REPORT NUMBER

9. SPONSORING/MONITORING AGENCY NAME(S) AND ADDRESS(ES)
Geophysics Laboratory
Hanscom AFB, MA 01731-5000
Contract Manager: Michael Hoke/OPI

10. SPONSORING/MONITORING AGENCY REPORT NUMBER
GL-TR-89-0326

11. SUPPLEMENTARY NOTES

12a. DISTRIBUTION/AVAILABILITY STATEMENT
Approved for public release; distribution unlimited

12b. DISTRIBUTION CODE

13. ABSTRACT *(Maximum 200 words)*

This report discusses several aspects of our studies of radiative transfer in the stratosphere. These include modifications to the SCRIBE instrument to enhance the 1250 cm^{-1} response and to improve its reliability. The results of a highly successful balloon flight on May 23, 1989 are discussed and a short interval in one of the spectra obtained is presented.

The analysis of data from the SCRIBE flight of July 5, 1984 as well as the data from two very high resolution solar interferometer flights are discussed. The analysis of the SCRIBE flight resulted in a daytime measurement of N_2O_5 variation. The high resolution data have yielded information on O_3 isotopic abundances in the stratosphere and also on improved line parameters for the O_3 bands in the 10 m region. The isotope studies have been published and two other papers have been accepted for publication. Keywords: Ozone, Nitrogen Oxides,

14. SUBJECT TERMS
Balloon instruments, Atmospheric measurements, Infrared Spectra (ind)

15. NUMBER OF PAGES
64

16. PRICE CODE

17. SECURITY CLASSIFICATION OF REPORT	18. SECURITY CLASSIFICATION OF THIS PAGE	19. SECURITY CLASSIFICATION OF ABSTRACT	20. LIMITATION OF ABSTRACT
Unclassified	Unclassified	Unclassified	SAR

TABLE OF CONTENTS

1. INTRODUCTION

The overall objective of this program has been the study of mid-infrared absorption and emission of the atmosphere at stratospheric altitudes. Emphasis has been placed on those frequencies where interactions with the major IR active gases (CO_2, H_2O, O_3 and CH_4) are minimal, i.e. the so-called windows.

The study consists of two main thrusts: 1) the evaluation of ultra high resolution transmission data obtained on balloon flights with a 2½ meter path difference Fourier Transform Solar Spectrometer; 2) the acquisition of stratospheric atmospheric emission data with the SCRIBE (Stratospheric Cryogenic Interferometer Balloon Experiment) system which, although of lower spectral resolution than the 2½ meter instrument, has sensitivity enough to monitor the low levels of radiation emitted by gases whose stratospheric concentrations can be of the order of a few parts per billion.

The ultra high resolution data relies on solar occultations to obtain long paths in the stratosphere and therefore is constrained to sunrise or sunset periods. The emission mode is applicable at any period and can be utilized for measurements of the diurnal variation of those compounds involved in the photochemistry of the stratosphere.

There is a continual need to improve the accuracy and detail of computational programs which model radiative transfer in the stratosphere. Data from both of the instruments discussed will provide input needed to assess the accuracy of the computation and permit further refinements.

2. WORK PERFORMED

2.1 SCRIBE

At the beginning of this contract the SCRIBE instrument was on loan to another Air Force program (designated as SCRIBE 99). As part of this program, a larger gondola was fabricated and a new interface panel was constructed. The system including these modifications was returned to the SCRIBE effort upon successful completion of the SCRIBE 99 operation in August, 1986.

The prime objective of the SCRIBE 99 flight required narrow field viewing at angles close to the Nadir. Once the major objective of the flight was accomplished, some data were recorded near the Earth's limb. It must be

recognized, however, that these data are far from optimum since the system was configured for viewing the high radiance earth surface rather than the much (three orders of magnitude or more) weaker atmospheric sources.

The instrument required some modification to the SCRIBE 99 configuration for atmospheric studies. The Dall-Kirkam telescope, utilized to narrow the instrument field, resulted in a 30% effective emissivity for the external optics. Although this was inconsequential compared to the upwelling radiances it could not be tolerated in atmospheric studies. The telescope therefore was replaced with a coolable plane mirror expected to reduce this extraneous emission to levels comparable with those due to the ZnSe window.

2.1.1 Flight Objectives

Photochemical modeling predicts a buildup of N_2O_5 in the stratosphere during the hours of darkness and a subsequent decay during the sunlight hours. Experimental verification of the concentrations reached and the rate of daylight decay are very sparse, consisting of one nocturnal emission measurement and a sunrise occultation measurement from the ATMOS satellite instrument. Previous SCRIBE flights in 1983 and 1984 were launched at sunrise to take advantage of the low surface wind conditions and were set up for maximum spectral coverage. As a result, data from these flights were not applicable to diurnal variation studies. A flight in 1985 was intended to make this measurement but due to loss of all command capability and a low float altitude (75K ft.) the data was of limited value.

The major emission feature of N_2O_5 occurs near 1245 cm^{-1}, well down on the high wavenumber tail of the stratospheric temperature blackbody emission curve. Adequate signal-to-noise ratios require lower NESR than needed for the HNO_3 measurements in the 900 cm^{-1} region. Given a source noise limited instrument the NESR can only be reduced by increasing the time of observation or by reducing the number of source photons which do not contribute to the desired signal.

The major source of photons in the stratospheric emission is the 667 cm^{-1} complex of CO_2 bands so reduction of the NESR could be achieved by a cold optical filter with strong attenuation at wavenumbers less than 900 cm^{-1}.

2.1.2 Instrument Modifications

A 2mm thickness of CaF_2 was installed behind the detector aperature in contact with the liquid helium heat sink. The resulting instrument response shows strong attenuation of photons below 800 cm^{-1}.

The previous gondola installation provided a scan through several zenith angles by tilting the entire cryostat. The procedure avoided the use of an external mirror and it's consequent emission, but the large mechanical advantage required to move the 1300 lb. cryostat made the process quite slow. The gondola system constructed for SCRIBE 99 mounted the instrument with the optical axis horizontal and controlled the viewing angle with a steerable plane mirror. The mounting system and mirror pedestal were preserved for atmospheric measurements, but the mirror size was reduced and a rotation mechanism designed to sequence through a set of 8 pre-selected viewing angles was fabricated. The system advanced by one step per command and then returned to the original position after all steps were completed. The time required between steps was much less than a single interferometer scan. As noted, the use of the mirror does introduce a 2 to 3 per cent emissitivity into optics but the effect can be moderated to a degree by cooling the mirror. The mirror has no antifrost system so temperature must not be reduced below the ambient frost point. A servomechanism was employed to initiate cooling above the tropopause and to maintain the mirror at 200K.

The carriage drive is reversed near the maximum path difference at a selected level of the 5 cm LVDT output and near ZPD by the 1 cm LVDT output. The ZPD turnaround position varies by several laser fringes in a random manner and drifts several laser fringes with temperature. The random variation precludes direct coadding of the interferograms and the temperature drift could result in problems from the positional gain change. In addition both transducers have resulted in mechanical problems after transportation.

A system which eliminated the need for both the LVDTs was implemented using an optical switch for the ZPD turnaround and a laser fringe counter for scan length. The optical switch employed a PIN diode detector and an LED source. PIN diodes improve in performance at LN_2 temperature and the LED was tested by immersion in liquid nitrogen. The set up performed well at room temperature but the LED output dropped drastically on cooling. With the reduced LED output the system proved less stable than the LVDT system. (Apparently the immersed diode created it's own insulating bubble of gas when current was applied. Installed in the instrument the diode was tightly coupled to a large thermal mass and was unable to warm itself.) The 1 cm LVDT system was therefore reinstalled in preparation for a flight at HAFB.

The system was transported to HAFB in early May 1987. Initial cold tests of the system went well but on 22 May the IR channel preamp failed. The balloon group was committed to operations out of Roswell, New Mexico in early June, so the instrument was transported to Roswell after warmup and repair.

The transport produced a large drop in fiber optic throughput so it was necessary to replace the fiber on arrival in Roswell. It also became necessary to replace the detector but the system was checked out flight-ready on June 15.

Several scheduled launches were aborted due to high surface winds before the system was launched on 19 June. The interferometer drive failed a few seconds after the system was released from the launch vehicle. The reason for the drive stoppage was not clear; the gondola was subject to some unusual accelerations during the launch run but later examination did not reveal a mechanical reason for the failure. After all attempts to restart the drive (park/drive command cycling and power on/off commands) failed, the remainder of the flight was directed to optimum recovery. In the meantime flight tests of the auxiliary systems (mirror cooler, mirror positioner and gondola stabilization) were conducted. The instrument was recovered in excellent condition.

As noted above, examination of the interferometer after the return to Denver showed the carriage to be quite free. The drive did not function after power was applied, however, and several bad IC's were identified which resulted in a severe overload of the $\pm$ 15V supplies. Replacement of the chips removed the overload but still produced no scan. The LVDT oscillator was found to be inoperable and was replaced as were several capacitors in the circuit.

These changes returned the system to operation but it failed again after the power had been cycled a few times. The electronics had no provision for two detector operation which was contemplated for future flights and was extremely difficult to trouble shoot. It was decided to redesign the entire electronics package with provisions for a second channel. This also permitted upgrades of the system by taking advantage of improvements in technology such as CMOS digital IC's and 16 bit analog to digital converters.

Construction and checkout of the new system was completed in mid July 1988 and preliminary interfacing with the G.L. PCM package was completed in August and a flight was scheduled for late September.

The equipment arrived at HAFB on September 8 and flight preparations begun the the next day. Most checkouts went well but difficulty was experienced in the PCM interface. This was finally resolved and all calibrations and checkouts were completed on September 25th. A flight was scheduled for early morning on 27 September. High bay checks prior to departure for the launch site on the evening of the 26th showed a severe perturbation in the carriage drive. When efforts to eliminate the variation through modifications to the external drive circuit were unsuccessful, the flight was cancelled. Tests the following day showed the drive was "sticky", the friction was larger than normal and variable.

Tests in Denver with the instrument warm showed the currents required to move the carriage were high and varied with position of the carriage. The instrument was returned to Idealab for polishing and relubrication of the carriage ways. The KCl beamsplitter showed severe fracturing apparently caused by corrosion of the mounting rings. The time of occurrence of the fracture is unknown but must have occurred during the final warmup or during transportation.

A new beamsplitter was ordered but was not finished when the refurbished interferometer was returned. A spare beamsplitter was installed for testing with the option of being retained if it survived the temperature cycle or of being replaced by the new unit if it did not.

The refurbished drive showed an order of magnitude reduction in friction and much higher compliance to the drive servo. The currents required for a stable drive were so low the unit was somewhat more microphonic than usual but showed acceptable speed variation overall. After a successful cool down a flight at HAFB in mid May 1989 (normally a period of low stratospheric wind velocity) was scheduled.

The cool down and flight preparations at HAFB went very well and the system was flight-ready on 18 May. The launch window was constrained to the period from 2400 to 0100 because of the requirement for one hour minimum at float altitude before sunrise. This appears to be a period where surface conditions are not usually favorable to the launch of a large balloon. Several scheduled launches were cancelled due to high surface winds before the night of May 22 when the winds were marginally high but appeared to be decreasing with time. Launch operations were continued until 2330 MDT at which time the trend was still favorable so inflation was begun. The system

was launched at 0011 MDT on 23 May. The bubble height winds were near max acceptable but the layout direction was good and the launch relatively gentle. The interferometer quickly recovered from the launch perturbations and operated well throughout the flight. Atmospheric emission data was recorded until ~1030 MDT when the helium was exhausted and the detector began to warm. At this time all objectives of the flight had been accomplished and the remainder of the flight was conducted to facilitate recovery. The termination command was issued when the system was several miles north and west of Carlsbad, NM. Impact was in an accessible area and the gondola was returned to HAFB on the evening of the 23rd. The recovered package appeared to be in excellent condition.

2.1.3 Flight Results

A total of ten hours thirty minutes of data was recorded over the course of the flight. Ascent data was acquired with the field of view horizontal to provide straight forward altitude profiles to 30 kilometers.

After the float level of 98K ft. was established, elevation scans were initiated. The mirror was stepped through the eight preestablished elevation angles at intervals of 10 minutes per step. The sequence was repeated several times before the liquid helium was exhausted and the detector began to warm.

The azimuth stabilization system introduced microphonics in the interferometer drive when activated. The stabilization was commanded off except when required to rotate the field of view away from the solar azimuth. The absence of stabilization may require sorting of the data according to azimuth angles.

Post-flight examination of float altitude data show the expected resolution and good signal-to-noise. Figures 1 and 2 show the N_2O_5 and HNO_3 regions of a spectrum generated by averaging 15 individual spectra. In Figure 3 the same averaged spectrum is compared to a synthetic spectrum over the interval 945-955 cm^{-1}, dominated by the P branch of the 00011-10001 band of $^{12}C^{16}O_2$. The synthetic spectrum was generated with the University of Denver line-by-line computer code, using the AFGL HITRAN data base[2]. The pressure-temperature profile used in the calculation was based on data from a drop-sonde released from the payload shortly after it reached float altitude, as well as data obtained by the National Weather Service in El Paso the day of the flight. A constant CO_2 mixing ratio of 340 ppm/v was used in the simulation, and a residual background radiance of 0.06 microwatts/cm^2-sr-cm^{-1}

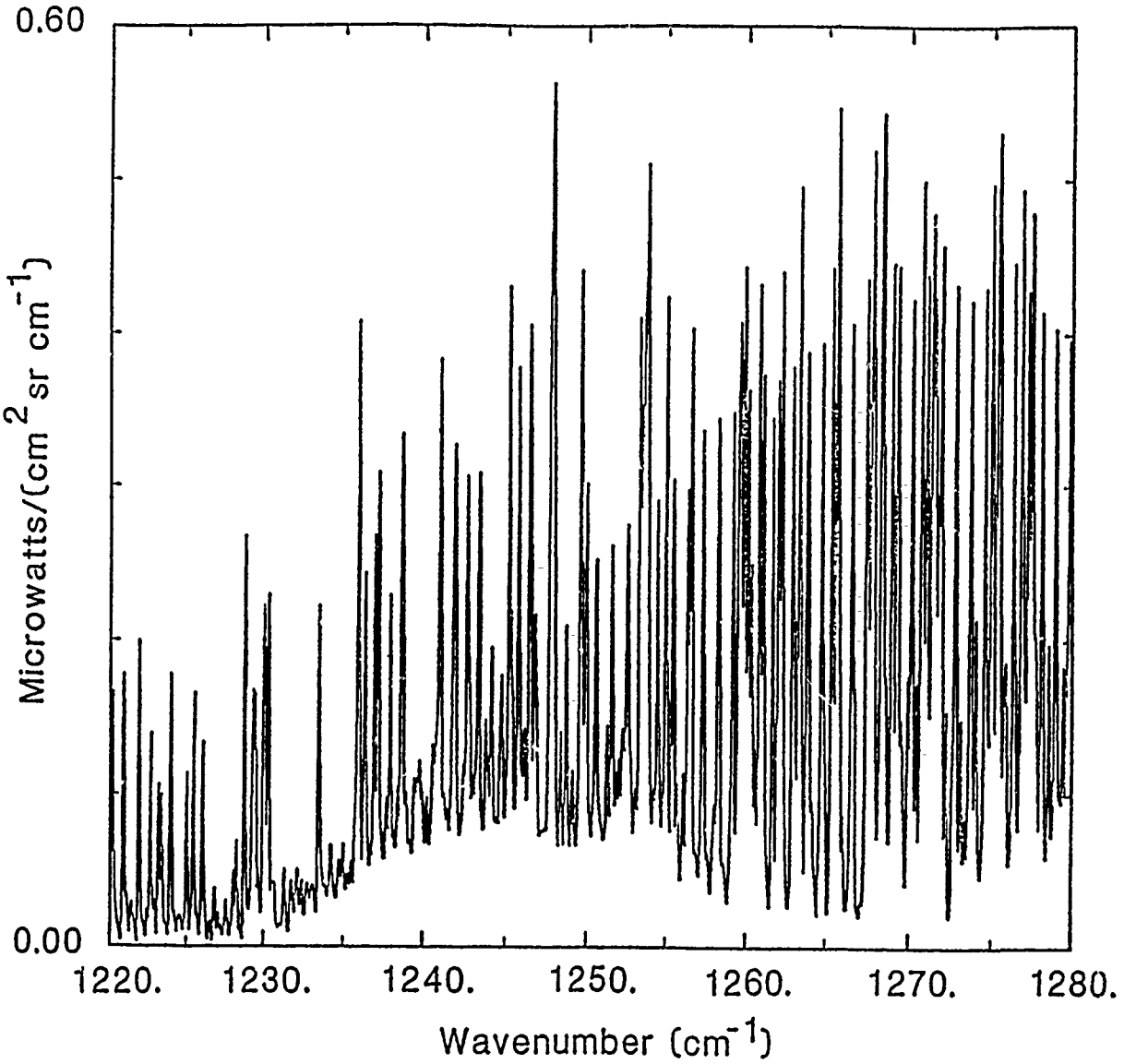

Fig. 1. A portion of the coadded spectrum generated by transformation of 15 interferograms recorded at 29.80 km altitude and a zenith angle of 92.70 degrees. Most of the line structure present is due to CH_4 and H_2O. The broad structure centered at 1245 cm^{-1} is due to N_2O_5.

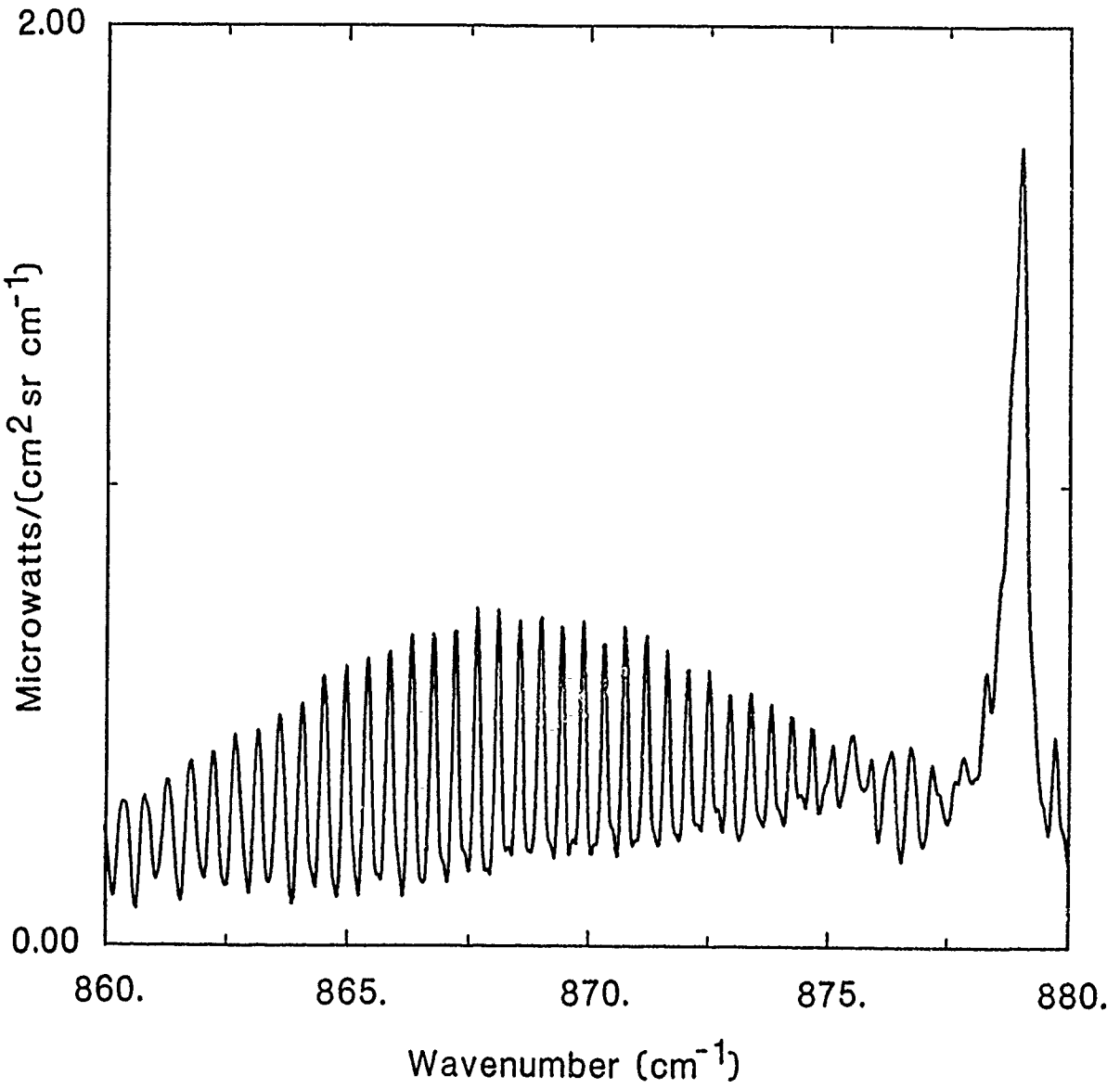

Fig. 2. The 870 cm^{-1} region from the same spectrum as the interval shown in Fig. 1. The predominent line complex is due to HNO_3.

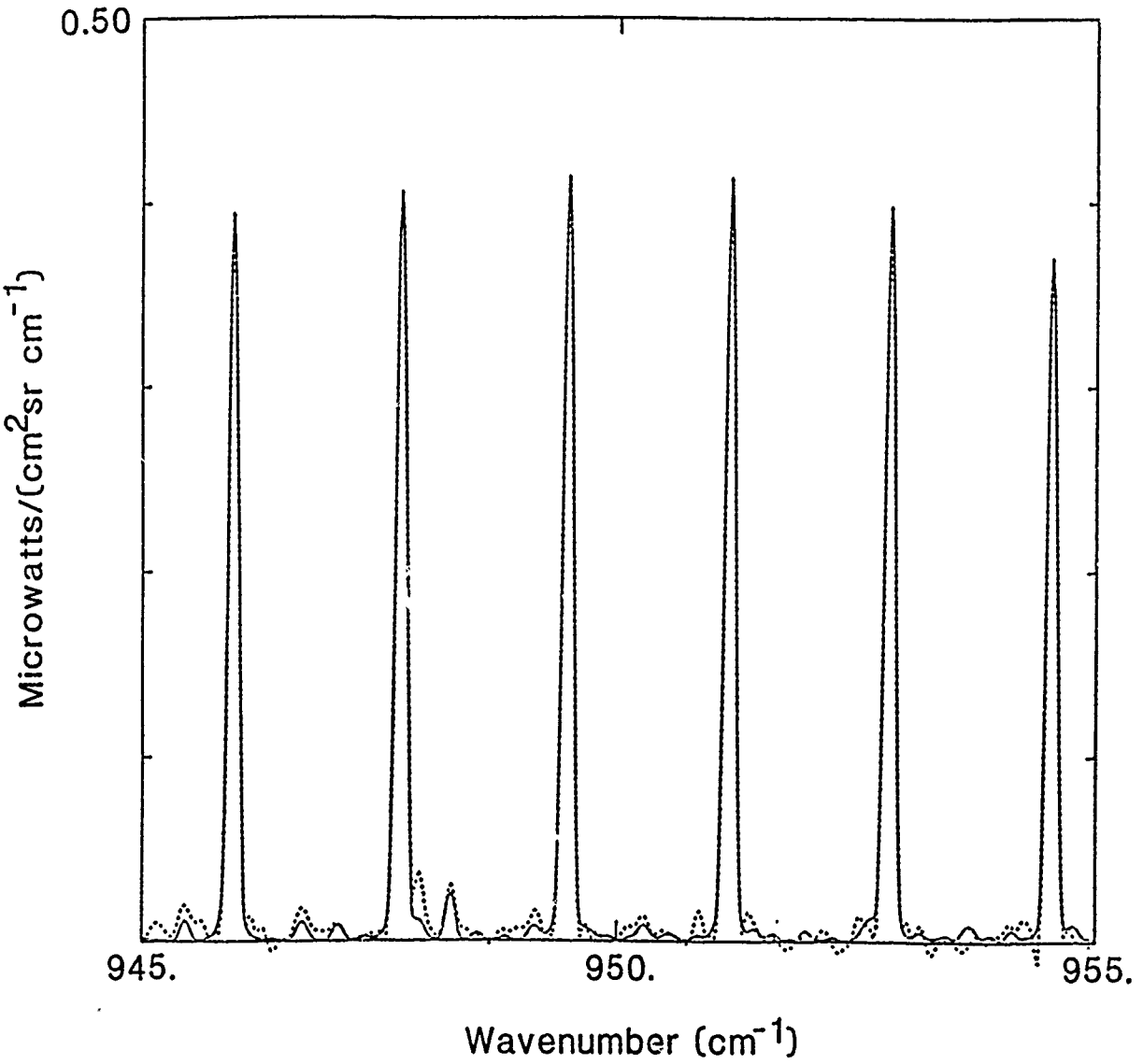

Fig. 3. Comparison in the 950 cm^{-1} region between a synthetic spectrum (solid line) and the experimental spectrum (dotted line) of Figs. 1 and 2.

was subtracted from the experimental spectrum. The largest discrepancy between the synthetic and observed spectrum occurs at 947.94 cm^{-1}, which is the center of the Q-branch of the ν_3 band of SF_6. Work is in progress to attempt to verify that this discrepancy is indeed due to stratospheric SF_6.

At least some of the spectra acquired at the higher solar elevation angles show some spurious radiation, possibly scattered sunlight. The data need to be analyzed further to identify the source of this radiation but it is not expected to seriously influence the retrieval of N_2O_5 concentration information. The data is being prepared for intensive analysis including the possibility of retrieving data on oxides of nitrogen other than HNO_3 and N_2O_5.

2.1.4 Analysis of Previous Data

The ultra high resolution solar interferometer has been successfully flown twice during the period covered by this contract. The data from these flights is being analyzed for potential inputs to the AFGL tapes. In addition, the effect of a myriad of very weak lines on the transmission in highly transparent regions for long stratospheric paths is being investigated.

The 5 July SCRIBE flight of 1984 did not reach float altitude until the sun was well above the horizon and the interferometer was configured for wide spectral coverage. Careful analysis of the data, however, reveals measurable radiances levels from N_2O_5. A paper on this measurement has been submitted to Journal of Geophysical Research.

2.2 HIGH RESOLUTION STUDIES

The data obtained with the SCRIBE system are limited in spectral resolution due to the low intensity of the atmosphere as a source of radiation. Our group at the University of Denver has also performed several balloon flights with a very high resolution solar spectrometer system. In the spectral region covered in these studies, the sun is a much more intense source and hence it is possible to study the atmospheric transmission at much higher resolution than achieved with the SCRIBE system. The solar spectrometer system also uses a moving mirror Michelson interferometer as the method of obtaining spectral data. The interferometer is optically coupled to a solar tracking system which maintains the solar radiation on the interferometer entrance aperture. The interferometer is capable of an unapodized spectral resolution of 0.002 cm^{-1}. The system is described in a paper submitted for publication[1]. While the spectral data have been obtained

on another program the spectral detail obtained in the region of the ozone absorption 960-1260 cm^{-1} is of particular interest in many systems designed for operation at high altitudes. Part of the effort on this contract has been to perform detailed analysis of the spectral features due to the many isotopic and "hot" bands of ozone. The studies have yielded information on the concentration of the various isotope's of ozone at high altitudes. In addition long low pressure path through the stratospheric ozone layer yields data on the many weak lines associated with the hot bands as well as those due to the normal isotope. Using all of these features and the theoretical analysis of the ozone spectrum by Flaud and Camy Peyret has yielded improved data on our understanding of the ozone absorption bands. The results of these analyses are presented in the two ozone publications listed.

3. REFERENCES

1. Murcray, F.J., J.J. Kosters, R.D. Blatherwick, J. Olson and D.G. Murcray, "High Resolution Solar Spectrometer System for Measuring Atmospheric Constituents," accepted for publication, Appl. Opt., 1989.

2. Rothman, L.S., R.R. Gamache, A. Goldman, L.R. Brown, R.A. Toth, H.M. Pickett, R. Poynter, J.-M. Flaud, C. Camy-Peyret, A. Barbe, N. Husson, C.P. Rinsland and M.A.H. Smith, "The HITRAN database: 1986 edition," Appl. Opt., 26, 4058-4097, 1987.

4. PUBLICATIONS RESULTING FROM WORK ON THIS CONTRACT

Blatherwick, R.D., D.G. Murcray, F.H. Murcray, F.J. Murcray, A. Goldman, G.A. Vanasse, S.T. Massie and R.J. Cicerone, "Infrared Emission Measurements of Morning Stratospheric N_2O_5," in press, 1989.

Flaud, J.-M., C. Camy-Peyret, C.P. Rinsland, V.M. Devi, M.A.H. Smith and A. Goldman, "Improved Line Parameters for Ozone Bands in the 10-μm Spectral Region," submitted to Appl. Opt., 1989.

Goldman, A., F.J. Murcray, D.G. Murcray, J.J. Kosters, C.P. Rinsland, J.-M. Flaud, C. Camy-Peyret and A. Barbe, "Isotopic Abundances of Stratospheric Ozone from Balloon-Borne High-Resolution Infrared Solar Spectra," J. Geophys. Res., 94, 8467-8473, 1989.

5. PERSONNEL

In addition to the authors, the following personnel have made significant contributions to this program:

John Van Allen, John Kosters, John Williams, Warren Cochran, Troy Dow, and Robert King.

Infrared Emission Measurements of Morning Stratospheric N_2O_5

R.D. Blatherwick, D.G. Murcray, F.H. Murcray, F.J. Murcray,
and A. Goldman
Department of Physics, University of Denver, Denver, Colorado 80208

G. A. Vanasse
Air Force Geophysics Laboratory, Bedford, Mass. 01731

S.T. Massie and R.J. Cicerone
National Center for Atmospheric Research, Boulder, Colorado 80307

Abstract

Infrared emission spectra obtained during a balloon flight of the AFGL SCRIBE system by the University of Denver are used to measure stratospheric N_2O_5 after sunrise over New Mexico (latitude 33 N). This is the first daytime measurement of N_2O_5. Comparisons with photochemical modeling show consistency between the observed and predicted decline of N_2O_5 during the morning hours.

Introduction

N_2O_5 is an important stratospheric reservoir species for NO_x, produced during the night by the reactions

$$NO_2 + O_3 \Rightarrow NO_3 + O_2 \quad (1)$$

$$NO_3 + NO_2 + M \Rightarrow N_2O_5 + M \quad (2)$$

After sunrise, N_2O_5 gradually photolyzes back into NO_2:

$$N_2O_5 + h\nu \Rightarrow NO_2 + NO_3 \quad (3)$$

$$\Rightarrow 2NO_2 + O \quad (4)$$

The diurnal variation of stratospheric N_2O_5, as computed in photochemical models (Brasseur and Solomon, 1984), is a periodic function; it decays due to photolysis after sunrise and increases through reaction (2) at night.

Nighttime N_2O_5 was tentatively observed by Roscoe (1982) and Evans (1986). A definitive observation of N_2O_5 was made by Toon et al. (1986) and Toon (1987) who observed the ν_{12} band (~1230-1260 cm^{-1}) and the ν_1 and ν_{11} bands (~1680-1770 cm^{-1}) in transmission spectra obtained with the ATMOS instrument at sunrise. Recently, Kunde et al.(1988) have measured nighttime N_2O_5 from infrared emission spectra in the ν_{12} region.

In the present work, infrared emission data are analyzed to demonstrate the first measurement of daytime N_2O_5, and the results are compared with the predictions of a one dimensional

photochemical model.

Observations

The data were obtained during a balloon flight of the AFGL SCRIBE system (Stratospheric CRyogenic Interferometer Balloon Experiment) by the University of Denver from Roswell, NM on 5 July, 1984. The instrumentation consisted of a LN_2 cooled Michelson interferometer system employing cat's eye optics and having a maximum path difference of ~9 cm. The time for a single scan was ~30 sec, including a 5 sec fly-back. The field of view was ~0.8°. Data for the radiometric calibration of the emission spectra were recorded during the flight by occasionally moving an on-board black body into the instrument field of view. For a detailed discussion of the SCRIBE instrumentation, see Murcray et al. (1984).

The balloon was launched at 0610 MDT, and reached a float altitude of 30.6 km at 0740 MDT. Data were recorded at a number of zenith angles. Of these, the scans at 90.6° and 91.1° were selected as most suitable for the detection and measurement of daytime N_2O_5. The 90.6° data displayed here is actually the average of 14 individual scans selected from those recorded between 0751 and 0759 MDT, while the 91.1° data are the average of 12 scans recorded during the interval 0916 to 0923.5 MDT. Sunrise occurred at the balloon float altitude at approximately 0530 MDT, and at ground level at the local time of 4^h56^m MST.

Analysis and Results

The data were analyzed by comparison with synthetic spectra generated using a line-by-line computer program developed at the University of Denver. The program, which takes refractive effects into account through a ray-tracing routine, calculates transmittance or emission over a user-selected number of atmospheric layers at a net interval of 0.001 cm^{-1}. The 1986 edition of the HITRAN database (Rothman et al., 1987) is used as input to the program. Line parameters for N_2O_5 do not exist, but the absorption coefficients needed to compute the N_2O_5 contribution to the atmospheric emission are generated by the program using the absorption cross-sections for N_2O_5 which are also included in the HITRAN database. Finally, the computed radiances are degraded in resolution by convolution with an appropriate instrument line shape function.

Residual background radiance was present at both observation angles (0.06 and 0.08 μWatt cm^{-2} $ster^{-1}$/ cm^{-1} at 90.6° and 91.1° respectively). For the present analysis, the data were adjusted by applying a wavelength dependent correction, described by a linear function such that theory and observation agreed in the "mini-windows" centered at 1227.0 and 1267.07 cm^{-1}, and at the N_2O-CH_4 blend at 1268.31 cm^{-1}. These three positions are away from significant N_2O_5 absorption. The peak N_2O_5 cross section is 1.90×10^{-18} cm^2 at 1246 cm^{-1} (with no temperature correction), whereas the cross sections for the three calibration points are $\leq 1.5 \times 10^{-19}$ cm^2. Validity of the adjustment is apparent in the reasonable agreement

to the CH_4 spectrum longward of 1268 cm^{-1}, and insensitivity of the N_2O_5 quantification to the background radiance. Subsequently, a least squares fitting for N_2O_5 amounts over the 1240-1247 cm^{-1} interval (with N_2O and CH_4 fixed) was made. Recent measurements of N_2O_5 cross-sections (Cantrell et al., 1988b) show 1.79×10^{-18} and 1.82×10^{-18} cm^2 at 1246 cm^{-1} for 298 and 233K respectively. Due to the small differences in comparison to the (room temperature) HITRAN value, and the small temperature dependence, we did not adjust the HITRAN values.

The pressure-temperature profile used in these simulations was taken from a radiosonde ascent from White Sands Missile Range at 0800 MDT on the same day as the balloon flight. Mixing ratio profiles for the various constituents (except N_2O_5) are from Smith (1982).

Figures 1a and 1b show a comparison between the calculated (solid line) and observed (dotted line) emission for zenith angles of 90.6° and 91.1° respectively. (Tangent heights = 30.3 km and 29.4 km). The data have been smoothed by a triangular filter to 0.25 cm^{-1} resolution. The region is dominated by sharp emission lines of CH_4, N_2O, H_2O, and to a considerably lesser extent, CO_2. At lower zenith angles, there are also contributions from HNO_3 above ~1280 cm^{-1}, as well as from CF_4 (~1283 cm^{-1}) and $ClONO_2$ (~1292 cm^{-1}), but these molecules do not contribute appreciably at the zenith angles shown here. The broad, smooth emission feature in Figure 1a and 1b from 1230 to 1260 cm^{-1} is due to stratospheric N_2O_5. This can be seen from Figure 1c, which is the same as Figure 1a, except that no N_2O_5 has been included in the calculation. Figure 2 shows an

expanded plot of the N_2O_5 1220-1270 cm^{-1} region from Figure 1a and Figure 1c. Figure 3 presents the observed radiance at 90.6° and a theoretical calculation which only includes the contribution due to N_2O_5.

The synthetic spectra of Figure 1a and 1b were computed using N_2O_5 profiles of the same general shape as the solid curves of Figure 4, which were generated as described below, multiplied by a scaling factor. The triangles in Figure 4 show the resulting N_2O_5 mixing ratios, 1.26 and 1.04 ppb, at the tangent altitudes of the two scans, 30.3 and 29.4 km respectively. Theoretical N_2O_5 mixing ratios are 2.10 and 1.65 ppb for the corresponding times of 6^h55^m and 8^h20^m MST. The observed relative decrease in N_2O_5 is therefore 0.83, whereas the theoretical value is 0.79. The estimated accuracy of the absolute N_2O_5 measurements is ±45%. This is based on uncertainties in radiance calibration and pointing (10%), vertical slope of the theoretical N_2O_5 mixing ratios (10%), spectral line parameters (15%), and the N_2O, CH_4 profiles (10%). Error in the observed relative change is estimated as ±15% (due to partial cancellation of systematic errors).

The theoretical N_2O_5 mixing ratios curves were calculated by a 1d photochemical transport model (Cicerone et al., 1983). The time dependent calculation extended between 10 and 80 km altitude. The pressure-temperature profile was that mentioned above, and the solar declination of +23° and the latitude of +33° matched that for the balloon flight.

Reaction rates for 81 two and three body gas-phase processes, and 25 photolysis processes for 38 gaseous species, follow that of JPL

1987 (DeMore et al. 1987), but with the Cantrell et al. (1988b) equilibrium constant for reaction (2). At 30 km at a temperature of 231K, the Cantrell and JPL 1987 equilibrium constants differ by 27%. However, for the geometry of the July 5 observation, the rate of thermal decomposition of N_2O_5 is slower than the diurnal average of N_2O_5 photolysis by a factor of 78, so the influence of the revised equilibrium constant upon the N_2O_5 mixing ratio is small. The total odd-chlorine ($Cl + ClO + HOCl + ClONO_2 + HCl + ClO_2$) mixing ratios are 2.17 ppb and 2.61 ppb at 30 and 60 km respectively. The J-values at 30 km are 3.42×10^{-5} sec^{-1} and 5.78×10^{-5} sec^{-1} for N_2O_5 photolysis (reactions (3) and (4)) for 6^h55^m and 8^h20^m MST respectively. The albedo value was 0.35, and J is insensitive to changes in the albedo (e.g. J equals 5.62×10^{-5} sec^{-1} for an albedo of 0.25 at 8^h20^m).

Since N_2O_5 is but one member of the NO_y family ($N + NO + NO_2 + NO_3 + HNO_3 + HNO_4 + 2*N_2O_5 + ClONO_2$) the theoretical value of N_2O_5 is related to the total NO_y mixing ratio. For the theoretical curves of Figure 2, NO_y is equal to 15.0 and 14.3 ppb at 40 and 30 km, respectively. Observations of Russell et al. (1988) for May 1985, sunset, 30 N latitude indicate NO_y near 16.7 and 15.2 ppb at 40 and 30 km, roughly 11% higher than our 1d theoretical predictions.

The model N_2O_5 and NO_y profiles are reasonable, though they may not accurately represent the mixing ratio profiles of July 5, 1984, due to seasonal variations and model limitations. Differences between one and two dimensional models are illustrated, for example, in Figure 10-58 of WMO/NASA 1985, in which the two modeling techniques at 30 km estimate different amounts of NO_y, and presumably,

different amounts of N_2O_5. Despite such differences, the present measurement of the relative change of N_2O_5 during the morning hours is consistent with the temporal change of the 1d calculation. Our observed early morning decline in N_2O_5 concentration is also consistent qualitatively (see eqs. (1)-(4)) with measured early morning increases in both NO and NO_2 (e.g. Ridley et al., 1977; Flaud et al, 1988; Rinsland et al, 1988).

The present morning N_2O_5 results and the sunrise and nighttime N_2O_5 observations by Tocn et al. (1986) and Kunde et al. (1988), all report N_2O_5 mixing ratios in the 1 to 2 ppb range near 30 km altitude. One sees that our observed mixing ratios at 0755 MDT and 0920 MDT are ~60% smaller than the values predicted by our model. Kunde et al. (1988) showed that their observed nighttime N_2O_5 is 20-30% smaller in comparison to a (different) photochemical model. However, the relative decrease of 0.83 over the 1.5 hours between the observations is consistent with that of 0.79 predicted by the model. The relative decrease in N_2O_5 concentration during the morning can be approximated by $D = \exp(-J\,\Delta t)$, where J is the average N_2O_5 photolysis rate over the time interval Δt. With $J = 4\times10^{-5}$ sec^{-1} and $\Delta t = 1^h25^m$, $D = 0.81$, in good agreement with the detailed model results of 0.79. D is not sensitive to the actual N_2O_5 amount and thus the absolute difference between models and measurements of N_2O_5 is less important than the temporal variations.

Acknowledgments

Research at the University of Denver was supported in part by the

Air Force Office of Scientific Research (AFOSR) as part of AFGL task 2310G1, by NASA under grant NAG2-351 and NSF under grant ATM 87-11572. Acknowledgment is made to the National Center for Atmospheric Research, which is supported by the National Science Foundation, for computer time used in this research. Research at NCAR was supported in part by the NASA UARS program under contract S-10782-C.

References

Brasseur, G., and S. Solomon, Aeronomy of the Middle Atmosphere, D. Reidel, Hingham, MA., 1984.

Cantrell, C.A., J.A. Davidson, A.H. McDaniel, R.E. Shetter and J.G. Calvert, Infrared absorption cross sections for N_2O_5, Chem. Phys. Lett., 148, 358-363, 1988a.

Cantrell, C.A., J.A. Davidson, A.H. McDaniel, R.E. Shetter and J.G. Calvert, The equilibrium constant for $N_2O_5 <=> NO_2 + NO_3$; absolute determination by direct measurement from 243 to 397K, J. Chem. Phys., 88, 4997-5006, 1988b.

Cicerone, R.J., S. Walters and S.C. Liu, Nonlinear response of stratospheric ozone column to chlorine injections, J. Geophys. Res. 88, 3647-3661, 1983.

DeMore, W.B., M.J. Molina, S.P. Sander, D.M. Golden, R.F. Hampson, M.J. Kurylo, C.J. Howard and A.R. Ravishankara, Chemical kinetics and photochemical data for use in stratospheric modeling, Evaluation number 8, JPL Publication 87-41, 196 pp., Jet Propulsion Lab., Pasadena, CA., 1987.

Evans, Wayne F.J., Observations of the 8 μm N_2O_5 thermal emission feature in the stratosphere, Appl. Opt., 25, 1866-1868, 1986.

Flaud, J.-M., C. Camy-Peyret, J.W. Brault, C.P. Rinsland, and D. Cariolle, Nighttime and daytime variation of atmospheric NO_2 from ground-based infrared measurements, Geophys. Res. Lett., 15, 261-264, 1988.

Kunde, V.G., J.C. Brasunas, W.C. Maguire, J.R. Herman, S.T. Massie, M.M. Abbas, L.W. Herath, and W.A. Shaffer, Measurement of

nighttime stratospheric N_2O_5 from infrared emission spectra, Geophys. Res. Lett., 15, 11, 1177-1180, 1988.

Murcray, F.H., F.J. Murcray, D.G. Murcray, J. Pritchard, G. Vanasse, and H. Sakai, Liquid nitrogen-cooled Fourier transform spectrometer system for measuring atmospheric emission at high altitudes, J. Atm. Ocean. Tech., 1, 351-357, 1984.

Ridley, B.A., M. McFarland, J.T. Bruin, H.I. Schiff, and J.C. McConnell, Sunrise measurements of stratospheric nitric oxide, Can. J. Phys. 55, 212-221, 1977.

Rinsland, C.P., A. Goldman, F.J. Murcray, F.H. Murcray, R.D. Blatherwick and D.G. Murcray, Infrared Measurements of atmospheric gases above Mauna Loa, Hawaii, in February 1987, J. Geophys. Res. 93, 12,607-12,626, 1988.

Roscoe, H.K., Tentative observation of stratospheric N_2O_5, Geophys. Res. Lett., 9, 901-902, 1982.

Rothman, L.S., R.R. Gamache, A. Goldman, L.R. Brown, R.A. Toth, H.M. Pickett, R. Poynter, J.-M. Flaud, C. Camy-Peyret, A. Barbe, N. Husson, C.P. Rinsland, and M.A.H. Smith, The HITRAN database: 1986 edition, Appl. Opt., 26, 4058-4097, 1987.

Russell, J.M. III, C.B. Farmer, C.P. Rinsland, R. Zander, L. Froidevaux, G.C. Toon, B. Gao, J. Shaw, and M. Gunson, Measurements of odd nitrogen compounds in the stratosphere by the ATMOS experiment on Spacelab 3, J. Geophys. Res., 93, 1718-1736, 1988.

Smith, M.A.H., Compilation of atmospheric gas concentration profiles from 0 to 50 km, NASA Tech. Memo., No. 83289, 1982.

Toon, G.C., C.B. Farmer, and R.H. Norton, Detection of

stratospheric N_2O_5 by infrared remote sounding, Nature, 319, 570-571, 1986.

Toon, G., Reply: Detection of stratospheric nitrogen species, Nature, 330, 427, 1987.

World Meteorological Organization/NASA, Atmospheric Ozone 1985: Assessment of our understanding of the processes controlling its present distribution and change, World Meteorological Organization, Geneva, 1986.

Legends for Figures

Figure 1. Comparisons of observed (dotted curves) and calculated (solid curves) atmospheric emission spectra in the 1220-1320 cm^{-1} region. The spectra were obtained during a balloon flight made on July 5, 1984 by the University of Denver with the AFGL SCRIBE system from balloon float altitude of 30.6 km. Zenith angles and tangent altitudes are indicated in the figure. The top two frames include N_2O_5 in the spectral calculations while for the bottom frame N_2O_5 was excluded from the calculation.

Figure 2. Comparison of observed (dotted curves) and calculated (solid curves) atmospheric emission spectra in the N_2O_5 1220-1270 cm^{-1} region. Frames (a) and (b) are an expanded version of (a) and (c) from Figure 1.

Figure 3. Observed emission spectra (dotted curves) and theoretical calculation (solid curve) only including the N_2O_5 contribution.

Figure 4. 1d Photochemical-transport model (see text) mixing ratio profiles (solid curves) of N_2O_5 for predawn (4^h40^m) and morning conditions used for comparison with the experiment. The triangles show the measured N_2O_5 mixing ratios 1.26 and 1.04 ppb, at the tangent altitudes 30.3 and 29.4 km.

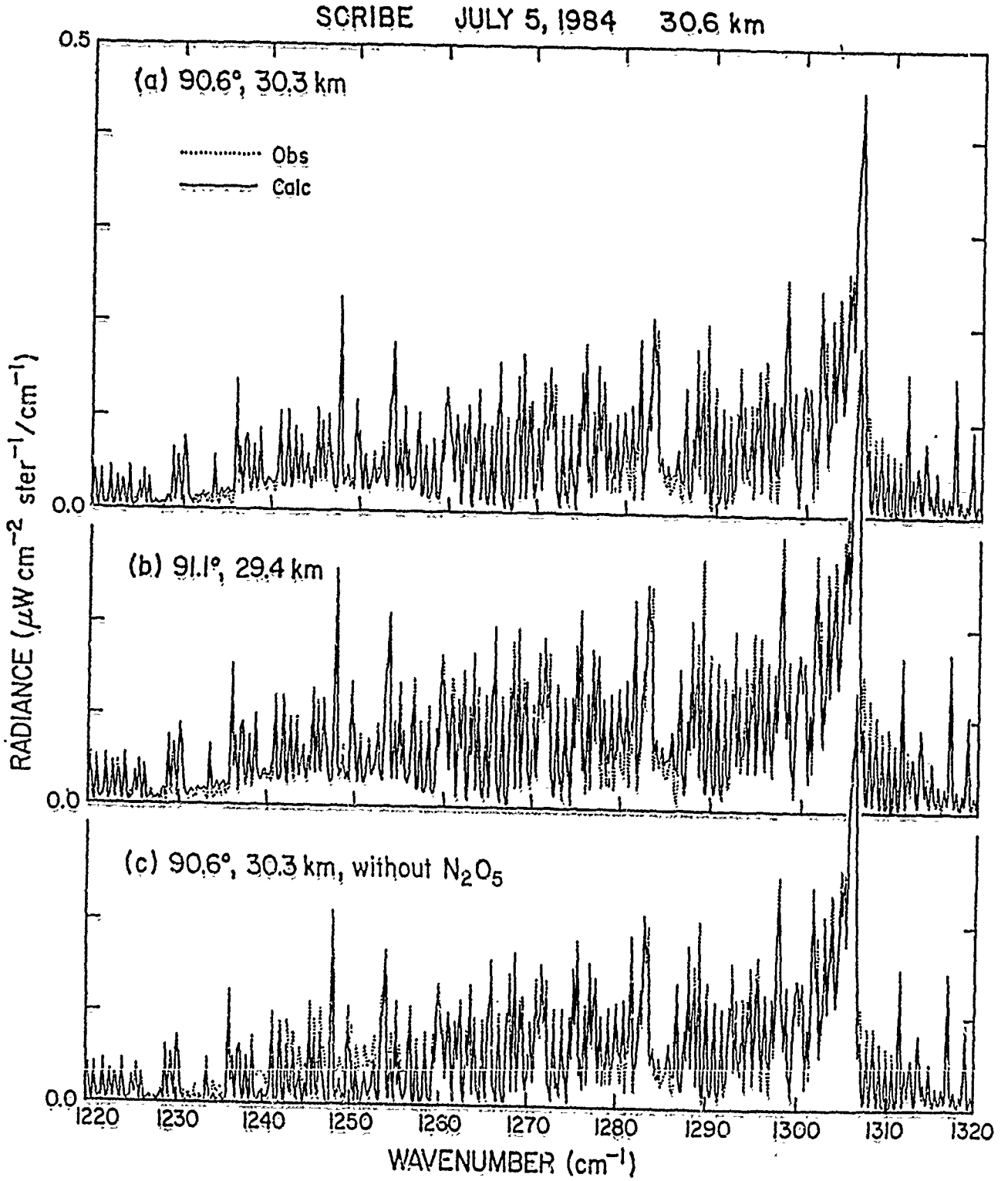
SCRIBE JULY 5, 1984 30.6 km
(a) 90.6°, 30.3 km
Obs
Calc
(b) 91.1°, 29.4 km
(c) 90.6°, 30.3 km, without N_2O_5
0.5
0.0
0.0
0.0
RADIANCE ($\mu W\,cm^{-2}\,ster^{-1}/cm^{-1}$)
1220
1230
1240
1250
1260
1270
1280
1290
1300
1310
1320
WAVENUMBER (cm^{-1})

Figure 1

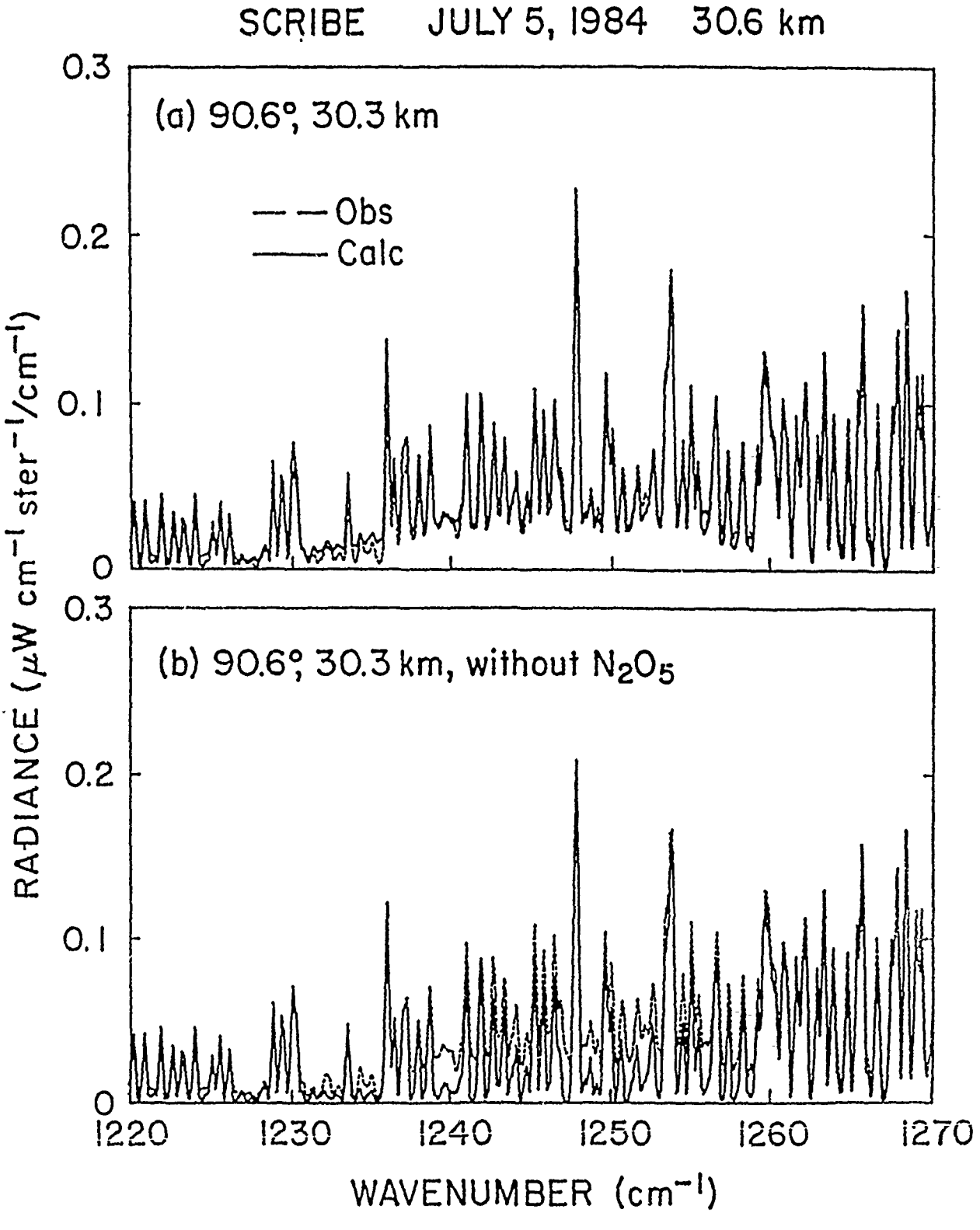
SCRIBE JULY 5, 1984 30.6 km
(a) 90.6°, 30.3 km
Obs
Calc
(b) 90.6°, 30.3 km, without N_2O_5
RADIANCE ($\mu W\ cm^{-1}\ ster^{-1}/cm^{-1}$)
0.3
0.2
0.1
0
1220
1230
1240
1250
1260
1270
WAVENUMBER (cm^{-1})

Figure 2

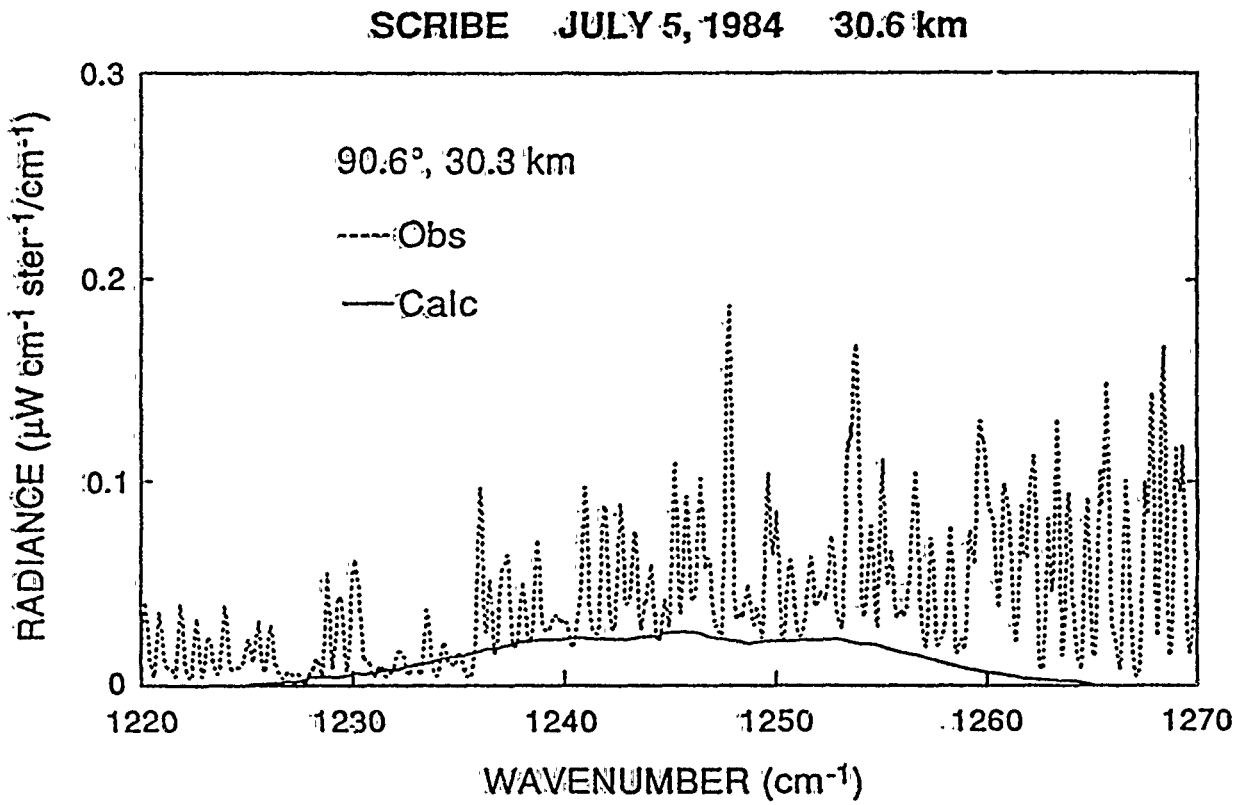
SCRIBE JULY 5, 1984 30.6 km
90.6°, 30.3 km
-----Obs
—Calc
RADIANCE (μW cm⁻¹ ster⁻¹/cm⁻¹)
0.3
0.2
0.1
0
1220
1230
1240
1250
1260
1270
WAVENUMBER (cm⁻¹)

Figure 3

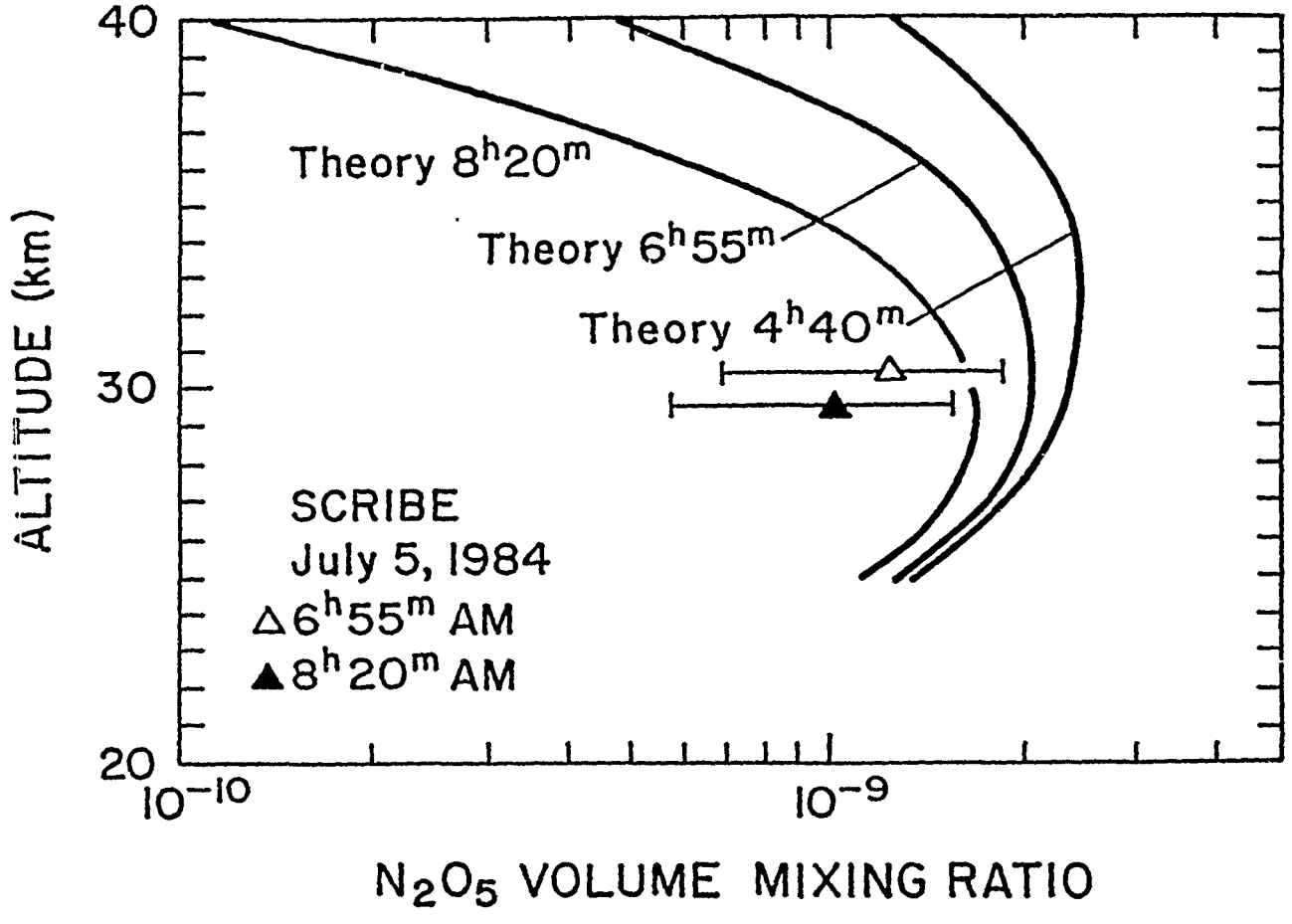
40
30
20
ALTITUDE (km)
Theory 8h20m
Theory 6h55m
Theory 4h40m
SCRIBE
July 5, 1984
△6h55m AM
▲8h20m AM
10−10
10−9
N2O5 VOLUME MIXING RATIO

Figure 4

Improved Line Parameters for Ozone Bands in the 10-μm Spectral Region

Jean-Marie Flaud, Claude Camy-Peyret, Curtis P. Rinsland, V. Malathy Devi,

Mary Ann H. Smith, and Aaron Goldman

V. Malathy Devi is with College of William and Mary, Physics Department, Williamsburg, Virginia 23185; A. Goldman is with University of Denver, Physics Department, Denver, Colorado 80208; J.-M. Flaud and C. Camy-Peyret are with Laboratoire de Physique Moléculaire et Atmosphérique, Tour 13, 3e étage, Université Pierre et Marie Curie et C.N.R.S., 4 place Jussieu, 75252 Paris Cedex 05 France; the other authors are with NASA Langley Research Center, Atmospheric Sciences Division, Mail Stop 401A, Hampton, Virginia 23665-5225.

Abstract

A complete update of spectroscopic line parameters for the 10-μm bands of ozone is reported. The listing contains calculated positions, intensities, lower state energies, air- and self-broadened halfwidths of more than 53,000 lines. The results have been generated using improved spectroscopic parameters obtained in a number of recent high-resolution laboratory studies. A total of 18 bands of $^{16}O_3$ (16 hot bands plus the ν_1 and ν_3 fundamentals) are included along with the ν_1 and ν_3 fundamentals of both $^{16}O^{16}O^{18}O$ and $^{16}O^{18}O^{16}O$. As shown by comparisons of line-by-line simulations with 0.003-cm^{-1} resolution balloon-borne stratospheric solar spectra, the new parameters greatly improve the accuracy of atmospheric calculations in the 10-μm region, especially for the isotopic $^{16}O^{16}O^{18}O$ and $^{16}O^{18}O^{16}O$ lines.

The need for improvements in the accuracy of remote sounding measurements of ozone in the Earth's atmosphere has motivated a number of recent studies devoted to the measurement and calculation of the spectrum of this molecule. In the infrared, the strongest bands are at 10 μm, where absorption is produced primarily by the ν_3 and ν_1 fundamentals of $^{16}O_3$. Hot bands of $^{16}O_3$ and the ν_3 and ν_1 bands of $^{16}O^{16}O^{18}O$ and $^{16}O^{13}O^{16}O$ also contribute significantly to the total absorption by ozone.[1] The 10-μm region has been used in a number of atmospheric studies of ozone, for example, the measurement of stratospheric O_3 profiles by the LIMS (Limb Infrared Monitor of the Stratosphere) instrument on the Nimbus 7 satellite,[2,3] measurements of ozone total columns inside the Antarctic ozone hole using high-resolution ground-based solar spectroscopy,[4] and the measurement of ozone isotope ratios from ground-based and balloon-borne high-resolution solar spectra.[5,6] Accurate knowledge of the absorption properties of the 10-μm ozone bands is also needed for climate models to estimate future changes in atmospheric and surface temperatures produced by the greenhouse effect.[7-9]

In the present paper, we report the calculation of improved line parameters for the ozone bands in the 10-μm region. In addition to revising the 8 bands on the 1986 HITRAN[10] and 1984 GEISA[11] line parameters compilations, the calculations have been extended to include 14 additional bands. For example, only four hot bands of $^{16}O_3$, the $\nu_1 + \nu_2 - \nu_2$, $\nu_2 + \nu_3 - \nu_2$, $\nu_1 + \nu_3 - \nu_1$, and $2\nu_3 - \nu_3$, were included previously,[10-12] with upper-state energy levels derived from spectra recorded at 0.02-cm^{-1} resolution.[13,14] The new parameters listing includes a total of 16 hot bands of $^{16}O_3$, based on extensive analysis of positions and intensities from 0.005- to 0.01-cm^{-1} resolution laboratory spectra. Also, for the first time, accurate parameters for the ν_1 and ν_3 bands of $^{16}O^{16}O^{18}O$ and $^{16}O^{18}O^{16}O$ are included. The ν_3 bands of both isotopic species appeared in the 1986

HITRAN and GEISA compilations,[10,11] but the crude approximations used to generate the linelist make the data unreliable for high-resolution studies. All of the new results have been derived from laboratory absorption spectra of ozone recorded with the McMath Fourier transform spectrometer operated on Kitt Peak by the National Solar Observatory.[15-24]

A summary of the new parameters is given in Table I. The integrated band intensities S_{band} have been evaluated without a minimum intensity cutoff applied in the computer code. This procedure gives the most accurate estimate for the integrated band intensity but includes many very weak lines not readily observable in long-path atmospheric or laboratory spectra. For this reason, the line listing was generated with minimum line intensity cutoffs of 1.0×10^{-25} cm^{-1}/molecule cm^{-2} at 296 K for the $^{16}O_3$ bands and 5.0×10^{-23} in cm^{-1}/molecule cm^{-2} at 296 K for the bands of the two ^{18}O-monosubstituted ozone isotopes. The sum of intensities in this list, denoted S_{list}, is also reported in Table I. The calculations include a scaling of the intensities by a multiplicative factor to convert the intensities from values for a pure isotopic species to values for a sample in natural isotopic molecular abundance. For this purpose, we adopted the isotopic ratios on the HITRAN compilation[10] ($^{16}O_3$=0.9929, $^{16}O^{16}O^{18}O$=0.0040, and $^{16}O^{18}O^{16}O$=0.0020). The differences between S_{band} and S_{list} are significant only for the very weak bands.

It should be noted that recent studies (see Ref. 6 and the references cited therein) have indicated that the isotopic abundances of the two ^{18}O-monosubstituted ozone isotopes are enhanced in the stratosphere as compared to the expected normal isotopic values. Therefore, atmospheric simulations generated with the new line parameters, which incorporate the natural abundance factors used in the HITRAN compilation,[10] may underestimate the absorption

produced by the $^{16}O^{16}O^{18}O$ and $^{16}O^{18}O^{16}O$ lines. The enrichment effect can be simulated by scaling the $^{16}O^{16}O^{18}O$ and $^{16}O^{18}O^{16}O$ line intensities by the appropriate isotopic enhancement factors in each atmospheric layer.

The calculations of the positions and intensities of the ν_3 and ν_1 fundamentals of $^{16}O_3$ and the two ^{18}O-monosubstituted ozone isotopes have been described previously.[15-17] Since only relative intensities could be determined from the laboratory spectra, it is important to recall the assumptions used in scaling the relative intensities to obtain absolute values. For $^{16}O_3$, a value of $(\partial\mu_z/\partial q_3)_e = -0.2662$ D was assumed, and for $^{16}O^{18}O^{16}O$, the intensities were computed by transferring the dipole moment of $^{16}O_3$ to $^{16}O^{18}O^{16}O$. The $^{16}O^{16}O^{18}O$ intensities have been calculated from relative intensities of $^{16}O^{16}O^{18}O$ and $^{16}O^{18}O^{16}O$ lines measured in the experimental spectra.[15] The amount of $^{16}O^{18}O^{16}O$ in the cell was first determined by comparing the measured relative intensities of the $^{16}O^{18}O^{16}O$ lines with the computed absolute values.[17] This amount was then multiplied by a factor of 2 to account for the difference in the relative concentrations of $^{16}O^{16}O^{18}O$ and $^{16}O^{18}O^{16}O$.

The line positions for the hot bands $\nu_2 + \nu_3 - \nu_2$ and $\nu_1 + \nu_2 - \nu_2$ of $^{16}O_3$ were computed from improved energy levels for the upper and lower states of both bands. The (011) and (110) energy levels were derived from analysis of the $\nu_1 + \nu_2$ and $\nu_2 + \nu_3$ bands in the 5.7-μm region.[18] The energy levels for the (010) state were calculated[20] from a refit to line positions measured in the ν_2 and $2\nu_2 - \nu_2$ bands.[19] The intensities of these hot bands were computed assuming transition moments derived from those of the ν_1 and ν_3 bands.

The line positions for the {(002),(101),(200)}-{(100),(001)} hot band system of $^{16}O_3$ were computed from improved energy levels derived for the $2\nu_3$, $\nu_1 + \nu_3$, and $2\nu_1$ bands in the 4.8-μm region[21] and the fundamental bands at 10 μm.[15] As

mentioned previously,[21] the observed energies of the (101) [19 2 17] and the (101) [45 3 42] rovibrational levels are displaced from their calculated values probably because of a resonance with an unidentified nearby level. The calculated energies of both levels were replaced with their observed values in generating the linelist. The intensities were computed from transition moments derived from those for the ν_3 and ν_1 bands and assuming the higher order dipole moment derivatives are equal to zero (except for the transition moment of (002)-(001) which was determined to be 0.5141×10^{-2} D from a least-squares fit of measured intensities).

Positions for the lines from the {(021),(120)}-(020) system have been calculated from energy levels of the $2\nu_2 + \nu_3$ and $2\nu_2 + \nu_3$ bands obtained from the recent first high-resolution analysis of these bands[22] and the constants for the (020) state reported by Flaud et al.[20] The intensities were computed assuming transition moments derived from those of the ν_1 and ν_3 bands.

Although the transitions are rather weak at atmospheric temperatures because of the Boltzmann factor, the {(012),(111),(210)}-{(110),(011)} system has been included to complete the description of the 10-μm region. The positions were calculated from upper-state energy levels determined from analysis of the $\nu_2 + 2\nu_3$, $\nu_1 + \nu_2 + \nu_3$, and $2\nu_1 + \nu_2$ bands in the 3.6-μm region[23] and lower-state energy levels determined from analysis of the $\nu_1 + \nu_2$ and $\nu_2 + \nu_3$ bands in the 5.7-μm region.[18] The intensity calculation has been performed assuming that the transition moments of (210)-(011) and (012)-(110) are equal to zero, and the other ones were derived from those of the ν_1 and ν_3 bands.

As an interim calculation, we have included air-broadened and self-broadened halfwidths based on empirical fits to recent laboratory measurements of ozone halfwidths.[24,25] The following expression has been adopted:

$$\alpha_L = a_0 + a_1 J'' + a_2 J''^2 + a_3 J''^3$$

where α_L is the Lorentz broadening coefficient at 296 K (in cm^{-1} atm^{-1} units) and J" is the lower state total angular momentum quantum number. For the air-broadened halfwidths, the coefficients $a_0 = 0.08735$, $a_1 = -0.0007447$, $a_2 = 6.08 \times 10^{-6}$, and $a_3 = 0.0$ have been used. On average, the measured air-broadened halfwidths in the ν_1 band[24] are about 10% larger than corresponding values on the 1986 HITRAN compilation.[10,26] The self-broadened halfwidths were calculated with the coefficients $a_0 = 0.11083$, $a_1 = -0.0016721$, $a_2 = 5.0084 \times 10^{-5}$, and $a_3 = -4.6741 \times 10^{-7}$ for $J'' \leq 25$. For $J'' > 25$ $\alpha_L = 0.093$ has been adopted. Self-broadened halfwidths were not included on the 1986 HITRAN[10] and 1984 GEISA compilations.[11]

The new ozone line parameters yield considerable improvement in the accuracy of high resolution atmospheric transmission and emission calculations in the 10-μm region, especially for the isotopic $^{16}O^{16}O^{18}O$ and $^{16}O^{18}O^{16}O$ bands and the hot bands of $^{16}O_3$. To illustrate the quality of the new line parameters, Figures 1 to 3 show comparisons of synthetic spectra with 0.003-cm^{-1} resolution stratospheric solar occultation spectra recorded with a balloon-borne Fourier transform spectrometer.[6,27,28] In all cases, the agreement between measurement and calculation is very good, even for the weakest lines. Figure 1 includes a comparison of the stratospheric spectra with a simulation of generated with the 1986 HITRAN compilation ozone line parameters.[10] The limitations of the previous data for high-resolution spectroscopic studies is obvious.

The new linelist also includes some significant changes in the distribution of the intensities within the stronger $^{16}O_3$ bands. An important example is the ν_1 band of $^{16}O_3$. Although the integrated intensity of the band in the new linelist is only slightly different (5.40×10^{-19} as compared to 5.56×10^{-19} cm^{-1}/molecule cm^{-2} at 296 K in the 1986 HITRAN list[10]), the intensities of individual lines selected for ozone retrievals from high-resolution atmospheric spectra are in most cases higher than on the 1986 HITRAN list,[10] resulting in correspondingly lower inferred ozone amounts.[29,30] The retrievals with the new line parameters are in better agreement with correlative ozone measurements than those derived with the earlier linelist.[29,30] Note that changes in the $^{16}O_3$ line intensities have an important effect on the derivation of $^{16}O^{16}O^{18}O/^{16}O_3$ and $^{16}O^{18}O^{16}O/^{16}O_3$ isotopic enhancement ratios from high-resolution infrared spectra. The recent analysis of 0.003-cm^{-1} resolution stratospheric solar absorption spectra by Goldman et al.[6] determined these ratios using the line parameters reported in this paper.

To provide an overview of the structures and the relative intensities of the bands in the new linelist, Figure 4 presents plots of absorption line intensity (cm^{-1}/molecule cm^{-2} at 296 K units) on a base 10 logarithm versus wavenumber scale for each ozone band. The bands are ordered by increasing band center, starting at the top of the left column and ending at the bottom of the right column. The final plot (lower right) contains all the lines displayed in the same format. The irregular distribution of intensity versus wavenumber within the bands results from the numerous resonances, both smooth and localized, occurring between the interacting states.

The National Solar Observatory is operated by the Association of Universities for Research in Astronomy, under contract with the National Science

Foundation. Research at the College of William and Mary and at the University of Denver is supported under cooperative agreements with the National Aeronautics and Space Administration.

Research at the University of Denver was supported in part by the Air Force Office of Scientific Research (AFOSR) as part of AFGL task 2310G1.

References

1. A. Goldman, T. G. Kyle, D. G. Murcray, F. H. Murcray, and W. J. Williams, "Long Path Atmospheric Ozone Absorption in the 9-10-μ Region Observed from a Balloon-Borne Spectrometer," Appl. Opt. 9, 565 (1970).

2. E. E. Remsberg, J. M. Russell III, J. C. Gille, L. L. Gordley, P. L. Bailey, W. G. Planet, and J. E. Harries, "The Validation of NIMBUS 7 LIMS Measurements of Ozone," J. Geophys. Res. 89, 5161 (1984).

3. S. R. Drayson, P. L. Bailey, H. Fisher, J. C. Gille, A. Girard, L. L. Gordley, J. E. Harries, W. G. Planet, E. E. Remsberg, and J. M. Russell III, "Spectroscopy and Transmittances for the LIMS Experiment," J. Geophys. Res. 89, 5141, (1984).

4. C. B. Farmer, G. C. Toon, P. W. Schaper, J.-F. Blavier, and L. L. Lowes, "Stratospheric Trace Gases in the Spring 1986 Antarctic Atmosphere," Nature 329, 126 (1987).

5. C. P. Rinsland, V. Malathy Devi, J.-M. Flaud, C. Camy-Peyret, M. A. H. Smith, and G. M. Stokes, "Identification of ^{18}O-Isotopic Lines of Ozone in Infrared Ground-Based Solar Absorption Spectra," J. Geophys. Res. 90, 10719 (1985).

6. A. Goldman, F. J. Murcray, D. G. Murcray, J. J. Kosters, C. P. Rinsland, J.-M. Flaud, C. Camy-Peyret, and A. Barbe, "Isotopic Abundances of Stratospheric Ozone from Balloon-Borne High Resolution Infrared Solar Spectra," J. Geophys. Res. 94, 8467 (1989).

7. V. Ramanathan, R. J. Cicerone, H. B. Singh, and J. T. Kiehl, "Trace Gas Trends and Their Potential Role in Climate Change," J. Geophys. Res. 90, 5547 (1985).

8. R. E. Dickinson and R. J. Cicerone, "Future Global Warming from Atmospheric Trace Gases," Nature 319, 109 (1986).

9. D. P. Kratz and R. D. Cess, "Infrared Radiation Models for Atmospheric Ozone," J. Geophys. Res. 93, 7047 (1988).

10. L. S. Rothman, R. R. Gamache, A. Goldman, L. R. Brown, R. A. Toth, H. M. Pickett, R. L. Poynter, J.-M. Flaud, C. Camy-Peyret, A. Barbe, N. Husson, C. P. Rinsland, and M. A. H. Smith, "The HITRAN Database: 1986 Edition," Appl. Opt. 26, 4048 (1987).

11. N. Husson, A. Chedin, N. A. Scott, D. Bailly, G. Graner, N. Lacome, A. Lévy, C. Rossetti, G. Tarrago, C. Camy-Peyret, J.-M. Flaud, A. Bauer, J. M. Colmont, N. Monnanteuil, J. C. Hilico, G. Pierre, M. Loete, J. P. Champion, L. S. Rothman, L. R. Brown, G. Orton, P. Varanasi, C. P. Rinsland, M. A. H. Smith, and A. Goldman, "The GEISA Spectroscopic Line Parameters Data Bank in 1984," Annales Geophys. 4, 185 (1986).

12. J.-M. Flaud, C. Camy-Peyret, and L. S. Rothman, "Improved Ozone Line Parameters in the 10- and 4.8-μm Regions," Appl. Opt. 19, 655 (1980).

13. A. Barbe, C. Secroun, P. Jouve, C. Camy-Peyret, and J.-M. Flaud, "High Resolution Infrared Spectrum of the $\nu_2 + \nu_3$ and $\nu_1 + \nu_2$ Bands of Ozone," J. Mol. Spectrosc. 75, 103 (1979).

14. J.-M. Flaud, C. Camy-Peyret, A. Barbe, C. Secroun, and P. Jouve, "Line Positions and Intensities for the $2\nu_3$, $\nu_1 + \nu_3$, and $2\nu_1$ Bands of Ozone," J. Mol. Spectrosc. 80, 185 (1980).

15. J.-M. Flaud, C. Camy-Peyret, V. Malathy Devi, C. P. Rinsland, and M. A. H. Smith, "The ν_1 and ν_3 Bands of $^{16}O_3$: Line Positions and Intensities," J. Mol. Spectrosc. 124, 209 (1987).

16. J.-M. Flaud, C. Camy-Peyret, V. Malathy Devi, C. P. Rinsland, and M. A. H. Smith, "The ν_1 and ν_3 Bands of $^{16}O^{18}O^{16}O$: Line Positions and Intensities," J. Mol. Spectrosc. 118, 334 (1986).

17. C. Camy-Peyret, J.-M. Flaud, A. Perrin, V. Malathy Devi, C. P. Rinsland, and M. A. H. Smith, "The Hybrid-Type Bands ν_1 and ν_3 of $^{16}O^{16}O^{18}O$: Line Positions and Intensities," J. Mol. Spectrosc. 118, 345 (1986).

18. V. Malathy Devi, J.-M. Flaud, C. Camy-Peyret, C. P. Rinsland, and M. A. H. Smith, "Line Positions and Intensities for the $\nu_1 + \nu_2$ and $\nu_2 + \nu_3$ Bands of $^{16}O_3$," J. Mol. Spectrosc. 125, 174 (1987).

19. H. M. Pickett, E. A. Cohen, L. R. Brown, C. P. Rinsland, M. A. H. Smith, V. Malathy Devi, A. Goldman, A. Barbe, B. Carli, and M. Carlotti, "The Vibrational and Rotational Spectra of Ozone for the (0,1,0) and (0,2,0) States," J. Mol. Spectrosc. 128, 151 (1988).

20. J.-M. Flaud, C. Camy-Peyret, C. P. Rinsland, M. A. H. Smith, and V. Malathy Devi, "Line Parameters for $^{16}O_3$ Bands in the 7-μm Region," J. Mol. Spectrosc., 134, 106 (1989).

21. C. P. Rinsland, M. A. H. Smith, J.-M. Flaud, C. Camy-Peyret, and V. Malathy Devi, "Line Positions and Intensities of the $2\nu_3$, $\nu_1 + \nu_3$, and $2\nu_1$ Bands of $^{16}O_3$," J. Mol. Spectrosc. 130, 204 (1988).

22. C. P. Rinsland, M. A. H. Smith, V. Malathy Devi, J.-M. Flaud, and C. Camy-Peyret, The $2\nu_2 + \nu_3$ and $2\nu_2 + \nu_1$ Bands of $^{16}O_3$: Line Positions and Intensities," submitted to J. Mol. Spectrosc.

23. M. A. H. Smith, C. P. Rinsland, V. Malathy Devi, J.-M. Flaud, and C. Camy-Peyret, "The 3.6 μm Region of Ozone: Line Positions and Intensities," submitted to J. Mol. Spectrosc. (1989).

24. M. A. H. Smith, C. P. Rinsland, V. Malathy Devi, D. C. Benner, and K. B. Thakur, "Measurements of Air-broadened and Nitrogen-broadened Half-widths and Shifts of Ozone Lines near 9 μm," J. Opt. Soc. Am. B 5, 585 (1988).

25. M. A. H. Smith, C. P. Rinsland, and V. Malathy Devi, "Measurements of Self-Broadening of Ozone," paper TE11, Forty-fourth Symposium on Molecular Spectroscopy, Ohio State Univ., Columbus, OH (1989).

26. R. R. Gamache and L. S. Rothman, "Theoretical N_2-broadened Halfwidths of $^{16}O_3$," Appl. Opt. 24, 1651 (1985).

27. A. Goldman, F. J. Murcray, R. D. Blatherwick, J.J. Kosters, F. H. Murcray, D. G. Murcray, and C. P. Rinsland, "New Spectral Features of Stratospheric Trace Gases Identified from High Resolution Infrared Balloon-borne and Laboratory Spectra," J. Geophys. Res., in press (1989).

28. F. J. Murcray, J. J. Kosters, R. D. Blatherwick, J. Olson, and D. G. Murcray, "High Resolution Solar Spectrometer System for Measuring Atmospheric Constituents," submitted to Appl. Opt., 1989.

29. C. P. Rinsland, A. Goldman, F. J. Murcray, F. H. Murcray, and D. G. Murcray, "Infrared Measurements of Atmospheric Gases Above Mauna Loa, Hawaii, in February 1987," J. Geophys. Res. 93, 12607 (1988).

30. M. R. Gunson, C. B. Farmer, R. H. Norton, R. Zander, C. P. Rinsland, J. H. Shaw, and B.-C. Gao, "Measurements of CH_4, N_2O, CO, H_2O and O_3 in the Middle Atmosphere by the ATMOS Experiment on Spacelab 3," submitted to J. Geophys. Res.

Table I. Summary of O_3 Bands Included in the Calculations

Vibrational States				Calculated Intensities[b]		Number of
Upper	Lower	Isotope[a]	Band Center (cm^{-1})	S_{band}[c]	S_{list}[d]	Lines
012	110	666	929.8447	4.16×10^{-23}	3.29×10^{-23}	164
002	100	666	954.7535	3.33×10^{-21}	3.27×10^{-21}	951
111	110	666	988.9772	2.12×10^{-21}	2.10×10^{-21}	1342
012	011	666	999.5841	6.01×10^{-21}	6.00×10^{-21}	1603
101	100	666	1007.6470	6.25×10^{-20}	6.25×10^{-20}	2646
001	000	686	1008.4528	2.65×10^{-20}	2.65×10^{-20}	2095
021	020	666	1008.6618	1.50×10^{-20}	1.50×10^{-20}	1511
002	001	666	1015.8068	1.68×10^{-19}	1.68×10^{-19}	3137
011	010	666	1025.5914	4.64×10^{-19}	4.64×10^{-19}	3883
001	000	668	1028.1120	5.12×10^{-20}	5.12×10^{-20}	3827
001	000	666	1042.0840	1.41×10^{-17}	1.41×10^{-17}	7224
111	011	666	1058.7166	1.22×10^{-22}	6.38×10^{-23}	252
101	001	666	1068.7003	5.31×10^{-21}	5.24×10^{-21}	2558
100	000	686	1074.3076	4.54×10^{-22}	4.54×10^{-22}	888
120	020	666	1087.3041	2.72×10^{-22}	2.21×10^{-22}	820
210	110	666	1089.9162	8.85×10^{-23}	3.33×10^{-23}	177
100	000	668	1090.3541	4.07×10^{-21}	4.07×10^{-21}	4425
110	010	666	1095.3308	1.27×10^{-20}	1.27×10^{-20}	3885
200	100	666	1098.0179	3.37×10^{-21}	3.30×10^{-21}	2931
100	000	666	1103.1373	5.40×10^{-19}	5.40×10^{-19}	6766
200	001	666	1159.0712	8.42×10^{-21}	8.34×10^{-21}	2057
210	011	666	1159.6556	1.95×10^{-22}	1.65×10^{-22}	593

Notes:
a. 666 = $^{16}O_3$, 686 = $^{16}O^{18}O^{16}O$, 668 = $^{16}O^{16}O^{18}O$.
b. Intensities are in cm^{-1}/molecule cm^{-2} at 296 K units. Values are scaled to include the assumed natural molecular isotopic abundance of each species. See text.
c. Integrated band intensity calculated by summing the individual line intensities without a minimum intensity cutoff.
d. Sum of the intensities of all lines in linelist. The linelist was calculated with minimum intensity cutoffs. See text.

Figure Captions

Figure 1. Comparison of a 0.003-cm^{-1} resolution solar occultation spectrum and a simulation of the data generated including the 1986 HITRAN ozone line parameters[10] (upper panel) and a simulation of the data generated with new ozone line parameters (lower panel). In the each panel, the upper curve is the line-by-line simulation which has been displaced vertically by 0.2 for clarity. The lower curve shows a solar spectrum obtained at sunset on June 6, 1988, during a balloon flight from Palestine, Texas, conducted by the University of Denver atmospheric spectroscopy group. The spectrum (normalized to the highest intensity in the interval) was recorded with a Michelson interferometer from a float altitude of 36.85 km and at a solar astronomical zenith angle of 92.61°. The corresponding refracted tangent height is 30.27 km. Arrows and capital letters in the lower panel indicate examples of ozone spectral features produced by different vibration-rotation bands. The ozone isotopic species and vibrational bands corresponding to the marked features are A=$^{16}O_3$, (002)-(100); B=$^{16}O^{18}O^{16}O$, (001)-(000); C=$^{16}O_3$, (002)-(001); D=$^{16}O^{16}O^{18}O$, (001)-(000); E=$^{16}O_3$, (011)-(010); F=$^{16}O_3$, (101)-(100); G=$^{16}O_3$, (100)-(000); H=$^{16}O_3$, (001)-(000); and I=$^{16}O_3$, (021)-(020). The R28 line of the 00011-10001 band of $^{12}C^{16}O_2$ at 980.9132 cm^{-1} (marked by a solid circle in both panels) is the only significant non-O_3 absorption feature in this spectral interval.

Figure 2. Comparison of a 0.003-cm^{-1} resolution stratospheric solar occultation spectrum (same scan as shown in Fig. 1) and line-by-line simulations with the new ozone line parameters. The upper spectrum, which has been displaced vertically by 0.1 for clarity, shows the absorption computed for the $^{16}O^{16}O^{18}O$ isotopic species only. The feature near 1090.36 cm^{-1} is the Q branch of the ν_1

band. More than 300 lines are included in the calculations. The two lower pectra show a comparison of the measured solar spectrum (solid line) with a simulation of the absorption by all gases (open diamonds). The absorption in this region is due almost entirely to $^{16}O_3$ lines and the lines of the $^{16}O^{16}O^{18}O$ ν_1 band Q branch.

Figure 3. Comparison of a 0.003-cm^{-1} resolution stratospheric solar occultation spectrum (same scan as shown in Figs. 1 and 2) and a line-by-line simulation including the new ozone line parameters. A number of features of the (200)-(100) band of $^{16}O_3$ are identified.

Figure 4. Absorption line intensity (cm^{-1}/molecule cm^{-2} at 296 K units) on a base 10 logarithm versus wavenumber scale for each ozone band. A plot with all of the lines in presented in the same format at the bottom of the right column.

Figure 1

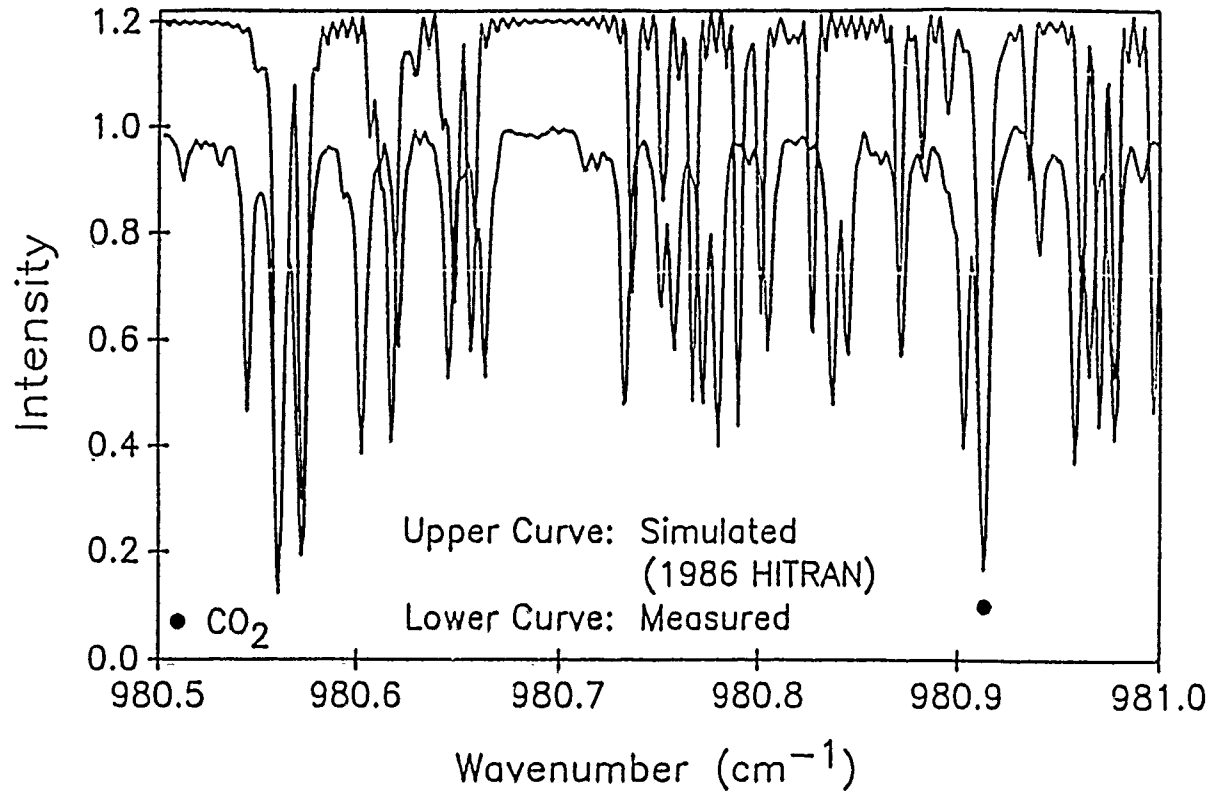
Intensity
1.2
1.0
0.8
0.6
0.4
0.2
0.0
980.5
980.6
980.7
980.8
980.9
981.0
Wavenumber (cm^{-1})
Upper Curve: Simulated
(1986 HITRAN)
Lower Curve: Measured
• CO_2

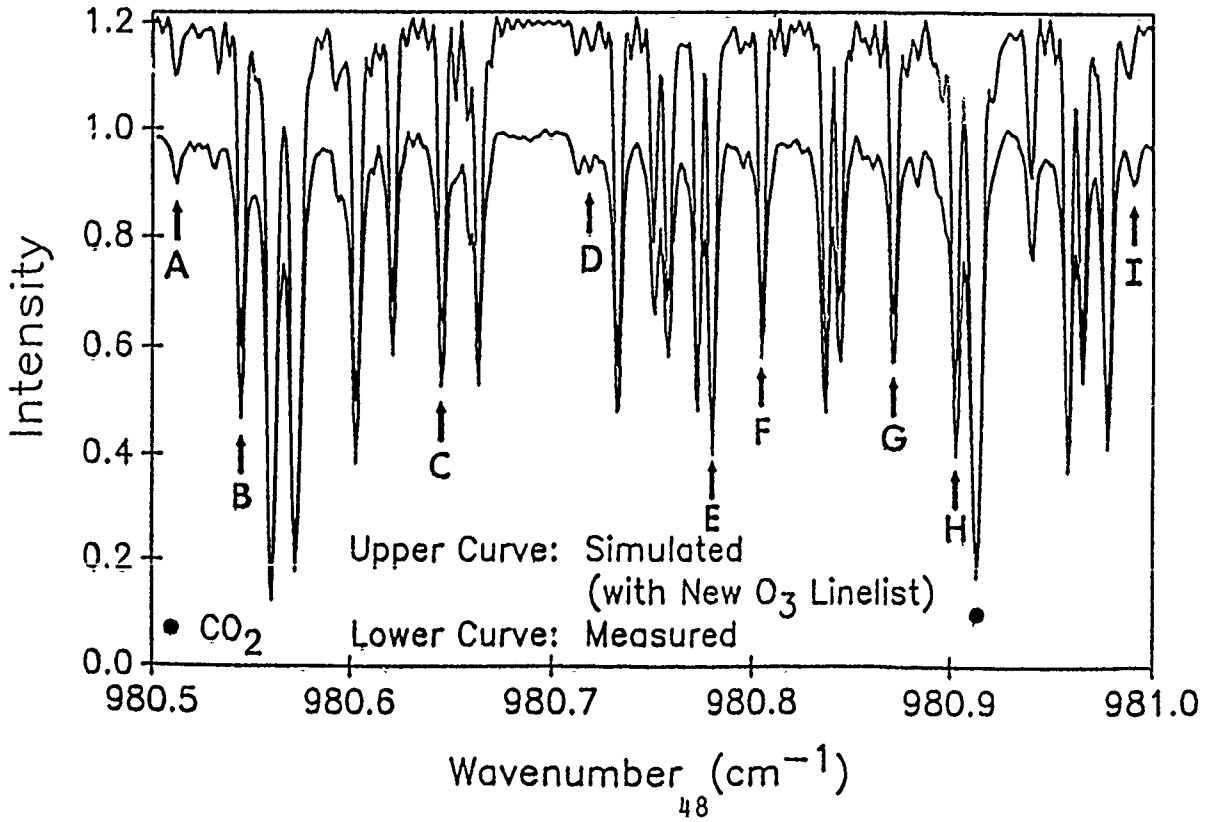
Intensity
1.2
1.0
0.8
0.6
0.4
0.2
0.0
A
B
C
D
E
F
G
H
I
980.5
980.6
980.7
980.8
980.9
981.0
Wavenumber (cm^{-1})
Upper Curve: Simulated
(with New O_3 Linelist)
Lower Curve: Measured
• CO_2

Figure 2

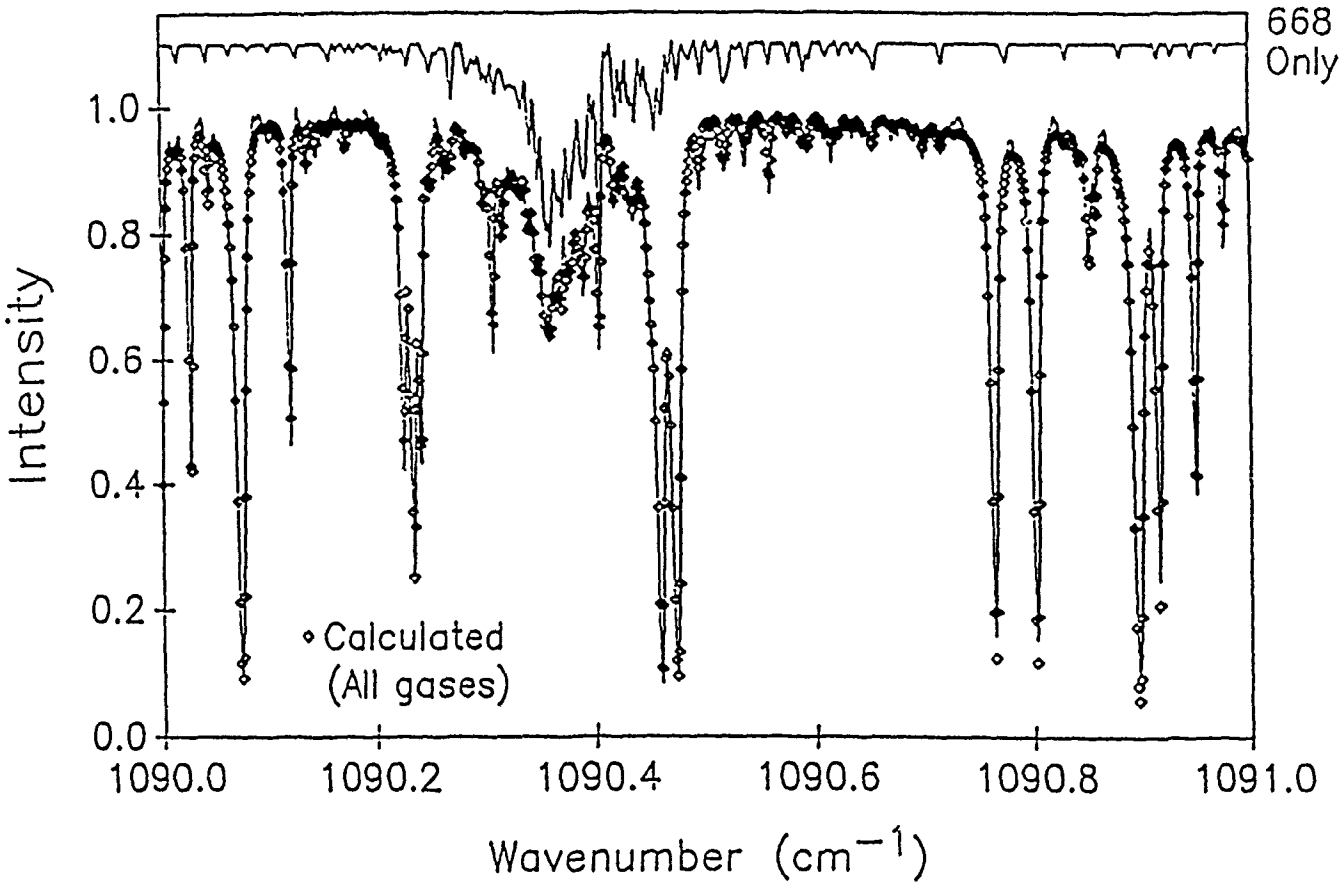
668
Only
Intensity
1.0
0.8
0.6
0.4
0.2
0.0
◇ Calculated
(All gases)
1090.0
1090.2
1090.4
1090.6
1090.8
1091.0
Wavenumber (cm⁻¹)

Figure 3

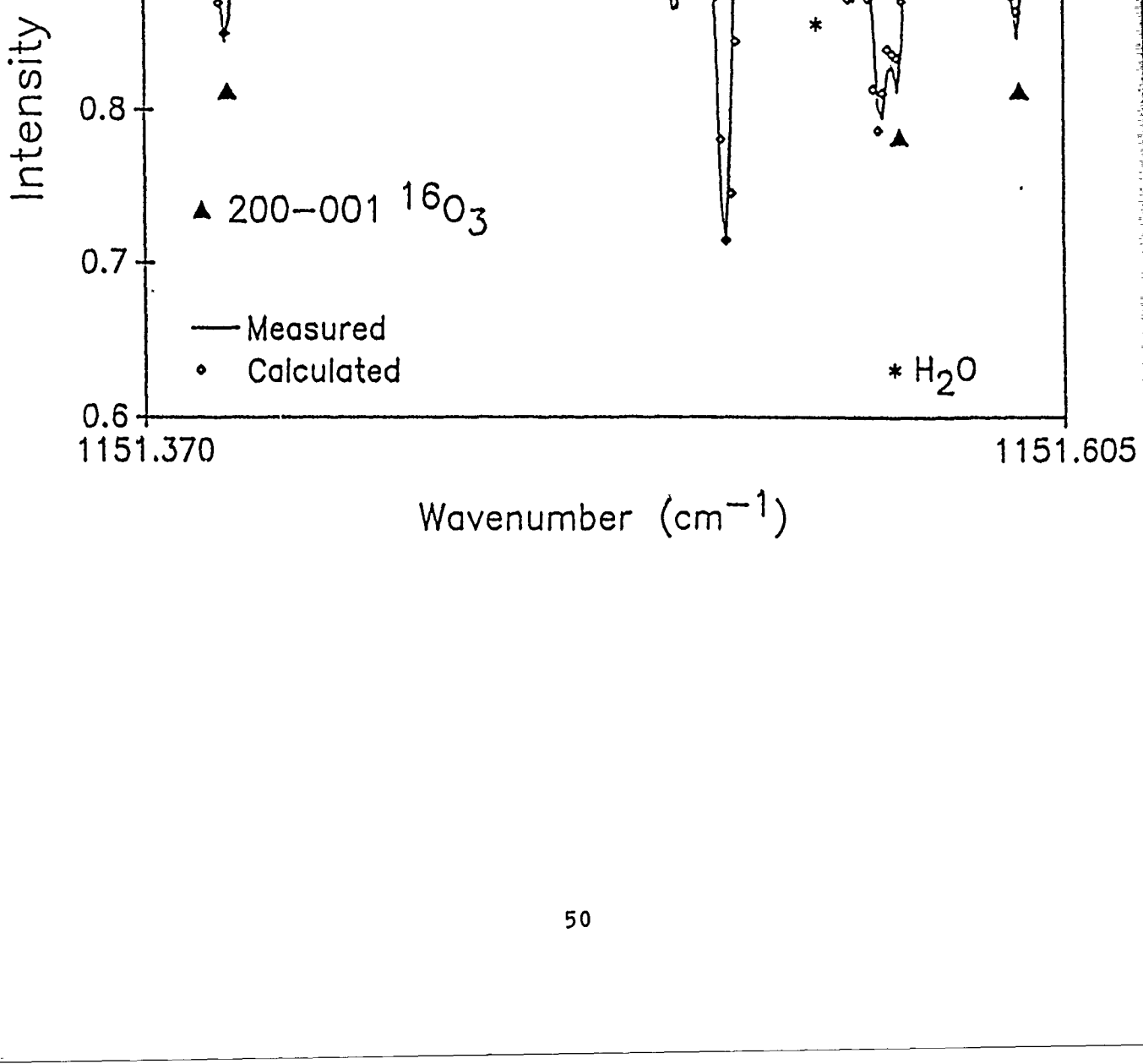
1.0
0.9
0.8
0.7
0.6
Intensity
▲ 200–001 $^{16}O_3$
Measured
Calculated
* H_2O
1151.370
1151.605
Wavenumber (cm^{-1})

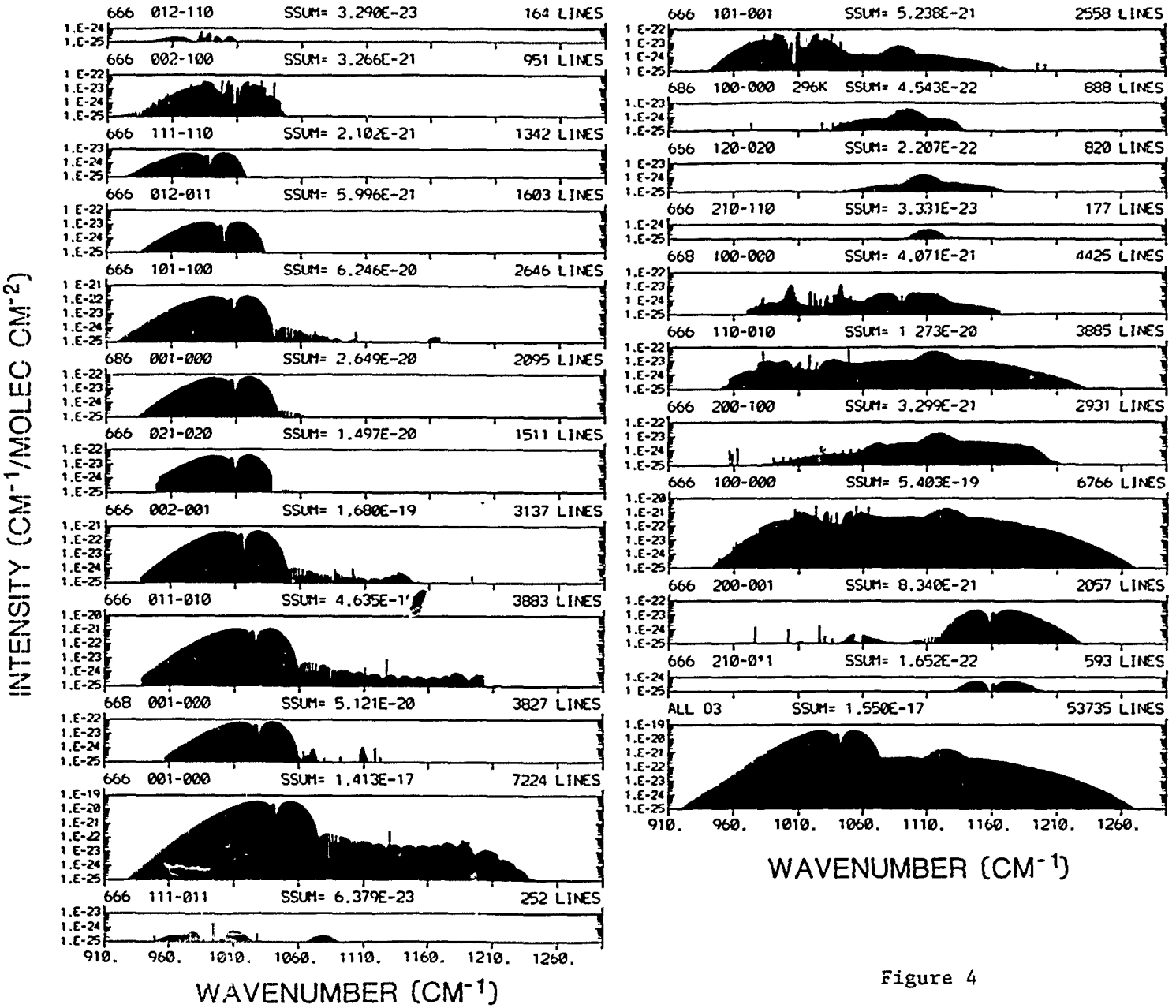
666 012-110 SSUM= 3.290E-23 164 LINES
666 002-100 SSUM= 3.266E-21 951 LINES
666 111-110 SSUM= 2.102E-21 1342 LINES
666 012-011 SSUM= 5.996E-21 1603 LINES
666 101-100 SSUM= 6.246E-20 2646 LINES
686 001-000 SSUM= 2.649E-20 2095 LINES
666 021-020 SSUM= 1.497E-20 1511 LINES
666 002-001 SSUM= 1.680E-19 3137 LINES
666 011-010 SSUM= 4.635E-1
668 001-000 SSUM= 5.121E-20 3827 LINES
666 001-000 SSUM= 1.413E-17 7224 LINES
666 111-011 SSUM= 6.379E-23 252 LINES
666 101-001 SSUM= 5.238E-21 2558 LINES
686 100-000 296K SSUM= 4.543E-22 888 LINES
666 120-020 SSUM= 2.207E-22 820 LINES
666 210-110 SSUM= 3.331E-23 177 LINES
668 100-000 SSUM= 4.071E-21 4425 LINES
666 110-010 SSUM= 1 273E-20 3885 LINES
666 200-100 SSUM= 3.299E-21 2931 LINES
666 100-000 SSUM= 5.403E-19 6766 LINES
666 200-001 SSUM= 8.340E-21 2057 LINES
666 210-0'1 SSUM= 1.652E-22 593 LINES
ALL 03 SSUM= 1.550E-17 53735 LINES
910. 960. 1010. 1060. 1110. 1160. 1210. 1260.
WAVENUMBER (CM-1)
INTENSITY (CM-1/MOLEC CM-2)

Figure 4

JOURNAL OF GEOPHYSICAL RESEARCH, VOL. 94, NO. D6, PAGES 8467-8473, JUNE 20, 1989

Isotopic Abundances of Stratopheric Ozone From Balloon-Borne High-Resolution Infrared Solar Spectra

A. GOLDMAN,[1] F. J. MURCRAY,[1] D. G. MURCRAY,[1] J. J. KOSTERS,[1]
C. P. RINSLAND,[2] J.-M. FLAUD,[3] C. CAMY-PEYRET,[3] AND A. BARBE[4]

Infrared solar absorption spectra recorded at 0.002-0.003 cm^{-1} resolution in the 10 μm region during two recent balloon flights from near 32°N latitude have been analyzed to determine the isotopic ratios of $^{16}O^{16}O^{18}O$ and $^{16}O^{18}O^{16}O$, the two most abundant forms of isotopically substituted ozone, relative to normal ozone, in the stratosphere. The analysis has used recent improvements in the line parameters for $^{16}O_3$, $^{16}O^{16}O^{18}O$, and $^{16}O^{18}O^{16}O$. Normalized to the standard isotopic ratios in ozone, the results show column-averaged isotopic enhancement ratios of 1.20 ± 0.14 and 1.40 ± 0.18 for $^{16}O^{18}O^{16}O/^{16}O^{16}O^{16}O$ and $^{16}O^{16}O^{18}O/^{16}O^{16}O^{16}O$, respectively, above 37 km altitude for flight measurements on November 18, 1987, and corresponding values of 1.16 ± 0.08 and 1.25 ± 0.12 for flight measurements on June 6, 1988. These measurements are the first such results obtained at high altitude using infrared techniques. The values are compared with heavy-to-normal O_3 ratios reported previously from other techniques.

INTRODUCTION

Cicerone and McCrumb [1980] first suggested that selective photodissociation of $^{16}O^{18}O$ relative to $^{16}O^{16}O$ may occur in the upper atmosphere and lead to an enhancement of the isotopic abundance of mass 50 ozone ($^{16}O^{18}O^{16}O$ and $^{16}O^{16}O^{18}O$) relative to $^{16}O_3$. Subsequently, *Mauersberger* [1981] reported nighttime mass spectrometer measurements of enriched heavy ozone in the stratosphere. Since these studies, there have been a number of theoretical and laboratory investigations as well as several in situ and remote sounding measurements of ozone isotopes in the stratosphere (see *Abbas et al.* [1987], *Kaye* [1987], *Thiemens and Jackson* [1987], *Bates* [1988], and *Anderson et al.* [1989] for recent discussions). At the present time there are difficulties in reconciling the stratospheric measurements which indicate the presence of sizable and variable enhancements in the amount of isotopically substituted ozone [*Mauersberger*, 1987; *Abbas et al.*, 1987] with theoretical calculations which predict negligibly small enhancements of heavy ozone [*Kaye and Strobel*, 1983; *Kaye*, 1986]. The possibility that the chemistry of stratospheric ozone formation and/or destruction may not be well understood could have important implications for upper atmosphere studies as a whole.

The possibility of detecting the two most abundant ^{18}O-monosubstituted varieties of ozone using high-resolution remote sounding techniques was first noted by *Goldman et al.* [1970]. In that study, simulations of O_3 absorption were compared to 0.5 cm^{-1} resolution long path balloon-borne solar spectra covering the 10-μm region. The ν_3 bands of the $^{16}O^{18}O^{16}O$ and $^{16}O^{16}O^{18}O$ species were shown to contribute significantly to the measured atmospheric absorption. Also, it was pointed out that a number of hot bands of $^{16}O_3$ are important absorbers in this spectral region. However, the low resolution of the atmospheric spectra and the very limited spectroscopic information available for O_3 at that time did not permit detailed spectroscopic analysis of the isotopic or hot band features in the atmospheric data. Balloon-borne solar spectra obtained later at 0.02 cm^{-1} resolution were used to improve the spectroscopic parameters for several of the important infrared atmospheric bands of normal ozone, but the spectroscopy of $^{16}O^{18}O^{16}O$ and $^{16}O^{16}O^{18}O$ remained crude [*Rothman et al.*, 1987]. Subsequent high-resolution laboratory studies in the far-infrared and middle infrared regions have produced major improvements in the line parameters for the pure rotation and the most important infrared bands of normal ozone and its ^{18}O-substituted isotopic varieties. These parameters have been used to identify and quantify $^{16}O^{18}O^{16}O$ and $^{16}O^{16}O^{18}O$ features in ground-based infrared solar absorption spectra [*Rinsland et al.*, 1985] and in balloon-borne far-infrared emission spectra of the stratosphere [*Abbas et al.*, 1987; *Carli and Park*, 1988].

On November 18, 1987, numerous infrared solar spectra were recorded at 0.002 cm^{-1} resolution during a balloon flight of a new Michelson Fourier transform spectrometer (FTS) operated by the University of Denver spectroscopy group The measurements were obtained on the ground prior to ascent, during ascent, and from the float altitude of 37 km during a flight from Fort Sumner, New Mexico. The spectra cover the 750- to 1350-cm^{-1} region with medium optical paths through the stratospheric ozone layer (the data collection stopped prematurely toward the end of the flight) and are rich in new detailed information on ozone absorption in the 10 μm region, with numerous well-isolated lines of the ν_1 and ν_3 bands of $^{16}O^{18}O^{16}O$ and $^{16}O^{16}O^{18}O$ and the ν_1 and ν_3 and various hot bands of $^{16}O_3$ prominent in the spectra. Accurate O_3 line positions, intensities, and air-broadened half widths, which have been derived recently from the studies of 0.005 cm^{-1} resolution laboratory measurements of pure ^{16}O-natural and ^{18}O-enriched ozone samples, allow assignments and detailed analysis of individual stratospheric lines of $^{16}O_3$, $^{16}O^{18}O^{16}O$, and $^{16}O^{16}O^{18}O$. A more recent balloon flight, made June 6, 1988, from Palestine, Texas, provided larger optical path solar spectra (from a float

[1]Department of Physics, University of Denver, Colorado.
[2]Atmospheric Sciences Division, NASA Langley Research Center, Hampton, Virginia.
[3]Laboratory of Molecular and Atmospheric Physics, Pierre and Marie Curie University, Paris.
[4]Faculty of Sciences, Reims University, Reims, France.

Paper number 89JD00600.
0148-0227/89/89JD-00600$05.00

altitude of 37 km), with the same instrument operating at 0.003-cm^{-1} resolution. The medium optical path spectra from this flight are consistent with the November 1987 flight spectra. Because of their higher quality, the new flight spectra allow a more accurate study of the normal and ^{18}O-monosubstituted lines of ozone.

In the present paper, selected portions of the measured spectra from both balloon flights will be presented along with comparisons of the measurements with line-by-line simulations in several narrow intervals. The equivalent width method for single lines and the nonlinear least squares spectral fitting method are used to quantify the observed isotopic enrichments, at high altitudes, of $^{16}O^{18}O^{16}O$ and $^{16}O^{16}O^{18}O$ relative to $^{16}O_3$.

Data Analysis

Figure 1 shows a sample of balloon flight spectra obtained at 0.02 (apodized) resolution with an older interferometer system [*Goldman et al.*, 1987]. Figures 2 and 3, plotted on the same wave number scale as Figure 1, show samples of the November 18, 1987, and the June 6, 1988, flights data, obtained with the new interferometer system, at 0.002 cm^{-1} and 0.003 cm^{-1} (unapodized) resolutions, respectively. The signal-to-rms noise ratio, which varies with wavelength, is approximately 100–200. Portions of these data have been reported in an atlas, with line positions and identifications [*Goldman et al.*, 1988]. The spectral details gained by the higher resolution are quite apparent. Individual lines of the heavy isotopic ozone species are all blended at 0.02 cm^{-1} resolution, but many are fully resolved in the new flight data. Line-by-line calculations with the HITRAN database [*Rothman et al.*, 1987] over the 970–1200 cm^{-1} region showed that even at medium optical path (such as the one obtained during the November 18, 1987, flight) all of the O_3 bands in this region require updating for proper spectral simulations of the new balloon flight data. Fortunately, recent laboratory and theoretical work provide most of the necessary parameters. The new line positions and intensities of ν_3, ν_1, $\nu_3 + \nu_2 - \nu_2$, $\nu_1 + \nu_2 - \nu_2$, $2\nu_3 - \nu_3$, and $\nu_1 + \nu_1 - \nu_1$ of $^{16}O_3$ and ν_3 and ν_1 of $^{16}O^{18}O^{16}O$ and $^{16}O^{16}O^{18}O$ are based on the recent work of *Flaud et al.* [1986, 1987], *Camy-Peyret et al.* [1986], *Malathy Devi et al.* [1987], *Rinsland et al.* [1988], and *Pickett et al.* [1988]. The natural ozone isotopic abundances of the 1986 HITRAN compilation [*Rothman et al.*, 1987, Table 4] have been assumed ($^{16}O_3$ = 0.9928, $^{16}O^{16}O^{18}O$ = 0.0040, $^{16}O^{18}O^{16}O$ = 0.0020 by volume) in our studies. New ozone air-broadened half widths have been calculated from coefficients derived from a fit to the experimental data of *Smith et al.* [1988]. These measured half widths are consistent with recent half width calculations [*Hartmann et al.*, 1988]. The new line parameters provide much improved agreement with the balloon data. However, the longer path spectra obtained during the June 6, 1988, flight show additional ozone lines not accounted for yet.

Figure 4 shows sample spectra and analysis of the R(14) 10.4 μm CO_2 laser line near 971.930 cm^{-1}. The narrow thermal core arising from absorption in the upper atmosphere and the pressure-broadened wings arising from absorption in the troposphere are quite distinct in the ground-based spectrum. Spectral least squares fitting of CO_2 lines with temperature sensitive line intensities have been used to derive the atmospheric temperature profile. However, the present study of the heavy O_3 enhancement relies on transitions with ground state energies such that the line intensities are nearly independent of the assumed atmospheric temperature profile.

Figure 5 shows a spectral least squares analysis of the 980.7–980.9 cm^{-1} interval, from the June 6, 1988, flight,

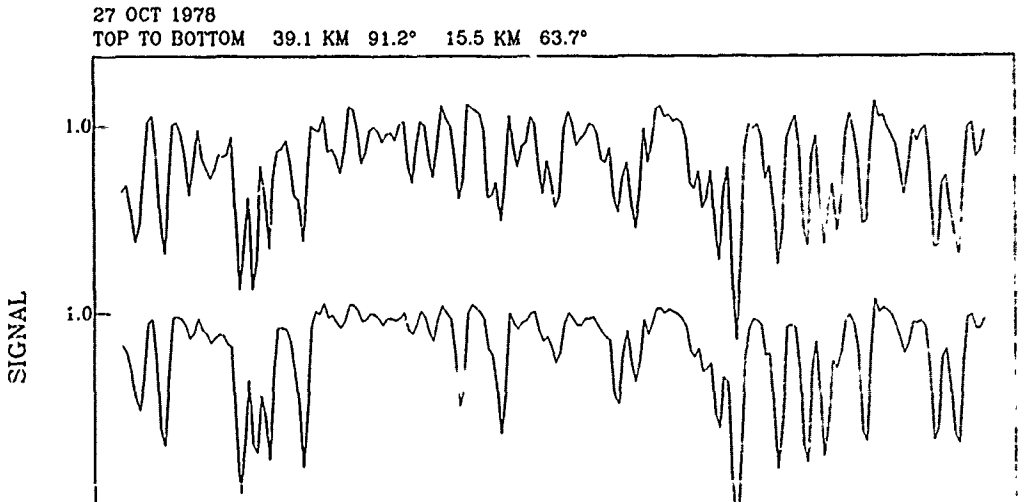

Fig. 1. Balloon-borne spectra in the 998- to 1000-cm^{-1} region, obtained on October 27, 1978, from Alamogordo, New Mexico, at 0.02-cm^{-1} resolution, with the University of Denver FTS interferometer. Altitudes and solar zenith angles are marked from top to bottom.

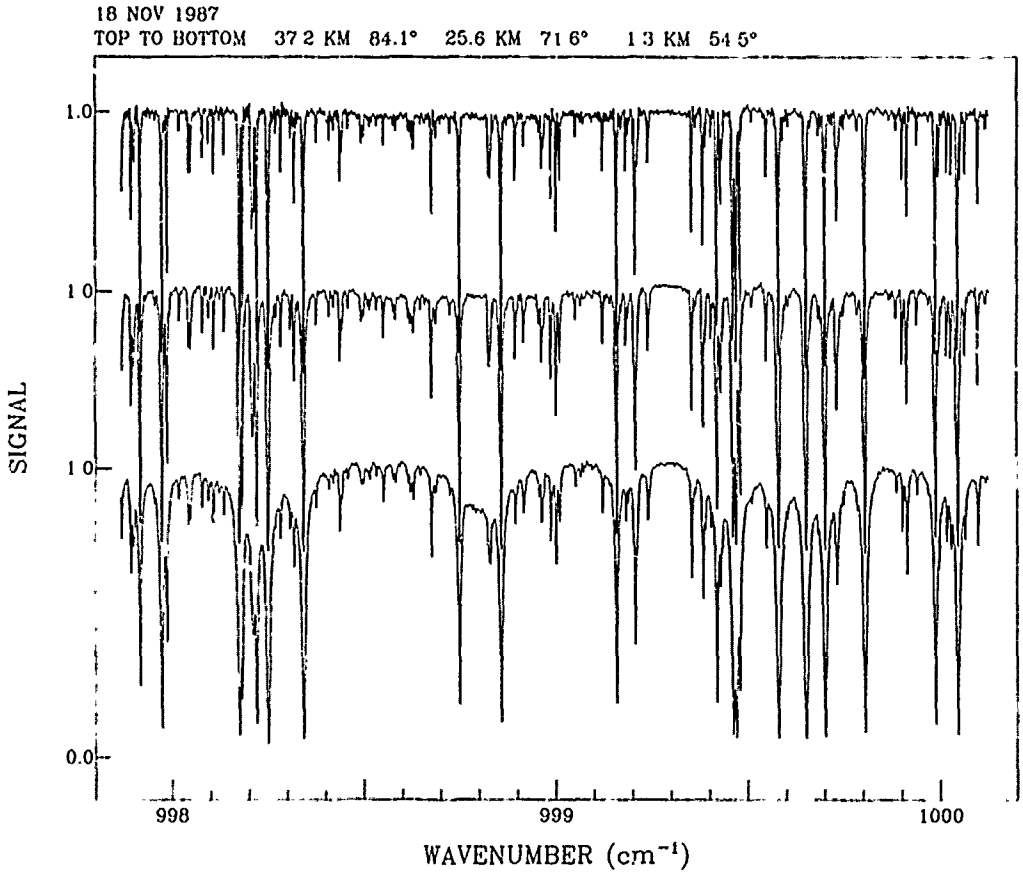

Fig. 2. Ground-based and balloon-borne spectra in the 998- to 1000-cm^{-1} region obtained on November 18, 1987, from Fort Sumner, New Mexico, at 0.002-cm^{-1} resolution, with the University of Denver FTS interferometer. Altitudes and solar zenith angles are marked from top to bottom.

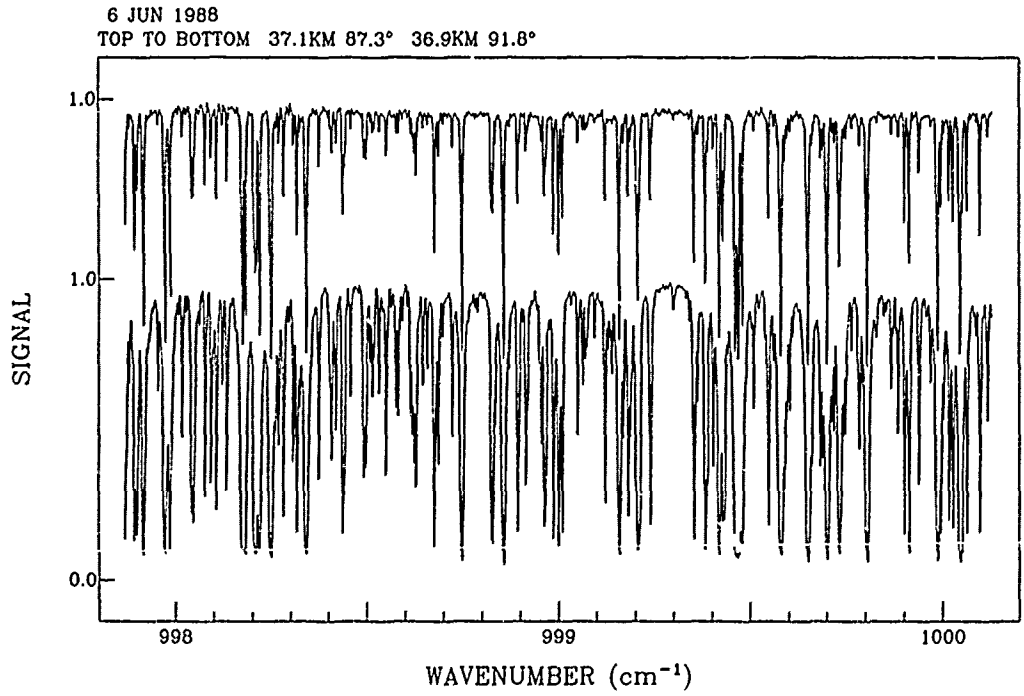

Fig. 3. Balloon-borne spectra in the 998- to 1000-cm^{-1} region, obtained on June 6, 1988, from Palestine Texas, at 0.003-cm^{-1} resolution, with the University of Denver FTS interferometer. Altitudes and solar zenith angles are marked from top to bottom.

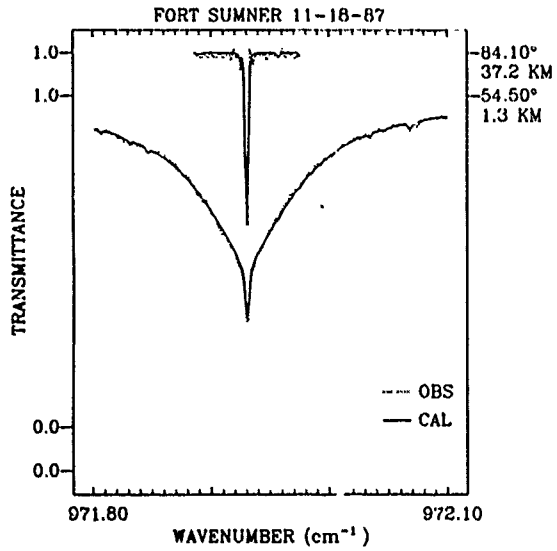

Fig. 4. The CO_2 R(14) 10.4 μm laser hot band line at 971.9303 cm^{-1} ($E'' = 1470.1192\ cm^{-1}$) as observed during the November 18, 1987, balloon flight from Fort Sumner, New Mexico. Spectral least squares fitting is used to derive the atmospheric temperature profile.

fitted assuming natural isotopic abundances for all O_3 species (only $^{16}O^{18}O^{16}O$ and $^{16}O^{16}O^{16}O$ are significant). Figure 6 demonstrates the corresponding analysis with $^{16}O^{18}O^{16}O$ and $^{16}O^{16}O^{16}$ fitted as two different species. Figure 7 is similar to Figure 6 but for the 1124.69–1124.83 cm^{-1} interval where only $^{16}O^{16}O^{16}O$ lines are apparent. Figure 8 shows a spectral least squares analysis of the 993.6–993.8 cm^{-1} interval from the November 18, 1987, flight. From such

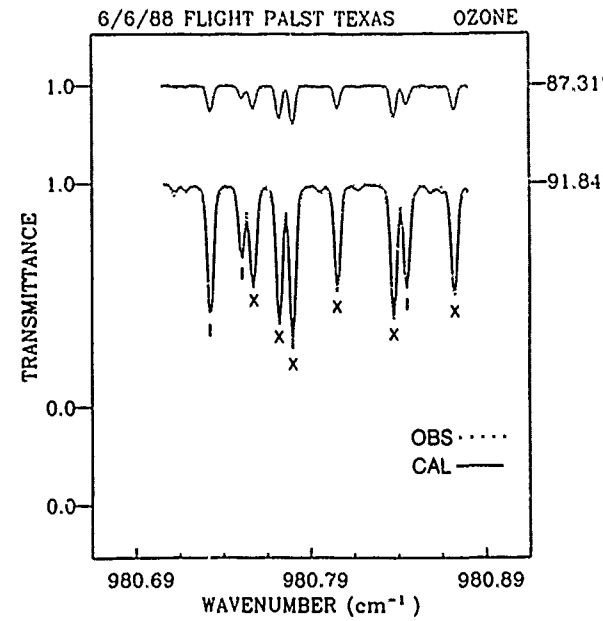

Fig. 6. Spectral least squares fitting of ground-based and balloon-borne solar spectra in the 980.70–980.90 cm^{-1} region. The spectra, at 0.003 cm^{-1} resolution, were obtained during a balloon flight on June 6, 1968, from Palestine, Texas, with the University of Denver FTS interferometer. The fit is for individual isotopic ozone abundances. The $^{16}O^{16}O^{16}O$ lines and the $^{16}O^{18}O^{16}O$ lines are marked with crosses and verticals, respectively.

analysis and from equivalent width analysis of weak lines the enhancements of $^{16}O^{18}O^{16}O$ and $^{16}O^{16}O^{18}O$ relative to $^{16}O^{16}O^{16}O$ have been determined. It is evident that both the high spectral resolution and the new ozone line parameters are crucial in this analysis

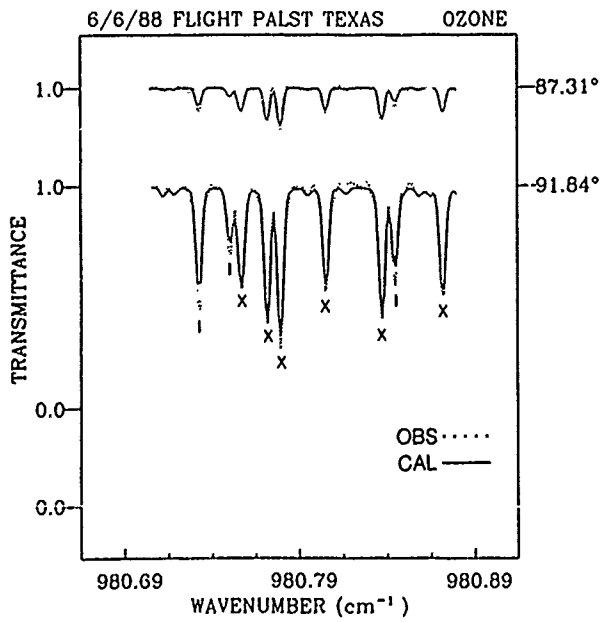

Fig. 5. Spectral least squares fitting of balloon-borne solar spectra in the 980.70–980.90 cm $^{-1}$ region. The spectra, at 0.003 cm $^{-1}$ resolution, were obtained during a balloon flight on June 6, 1988, from Palestine, Texas, with the University of Denver FTS interferometer. The fit assumes normal abundances of the isotopes of ozone. The $^{16}O^{16}O^{16}O$ lines and the $^{16}O^{18}O^{16}O$ lines are marked with crosses and verticals, respectively.

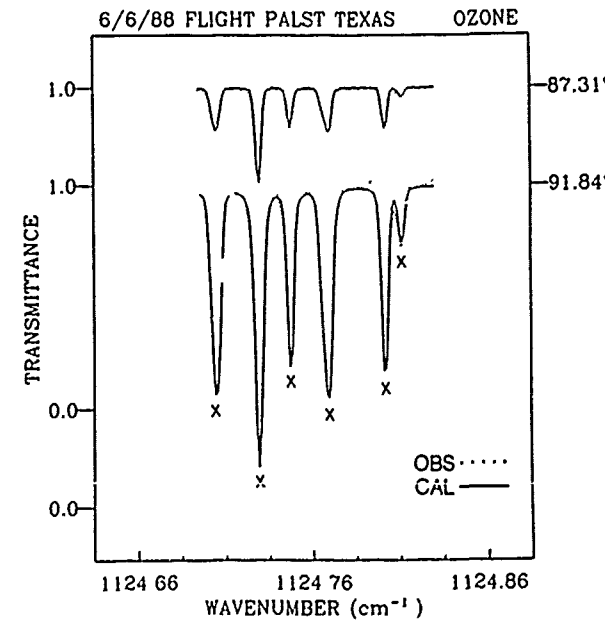

Fig. 7. Spectral least squares fitting of balloon-borne solar spectra in the 1124.69–1124.83 cm $^{-1}$ region. The spectra, at 0.003 cm $^{-1}$ resolution, were obtained during a balloon flight on June 6, 1988, from Palestine, Texas, with the University of Denver FTS interferometer. This interval is dominated by $^{16}O^{16}O^{16}O$ lines, marked with crosses.

Similar to *Rinsland et al.* [1985], we have selected $^{16}O^{18}O^{16}O$ lines in the 980–1002 cm^{-1} interval, $^{16}O^{16}O^{18}O$ lines in the 1042–1045 cm^{-1} interval, and $^{16}O^{16}O^{16}O$ lines in the 1100–1180 cm^{-1} interval. First, a high-altitude scan and a ground-based scan from November 18, 1987, were analyzed using the equivalent width method. Spectral least squares analysis was also performed for several intervals, to verify the validity of the weak line approximation and to include more O_3 lines in each interval. From these analyses, values of 1.20 ± 0.14 and 1.40 ± 0.18 were obtained for the enhancement ratios $^{16}O^{18}O^{16}O/^{16}O^{16}O^{16}O$ and $^{16}O^{16}O^{18}O/^{16}O^{16}O^{16}O$, respectively, above 37 km. The errors are dominated by the noise and residual distortions of the spectra, which limit the accuracy of the equivalent widths determination and the spectral fittings. The uncertainties in the new line parameters are only a small source of error. The ground-based spectrum shows the pressure broadening of the lower atmosphere ozone lines, many of which are overlapped by various tropospheric lines. As a result, within an error limit of ~20%, no enhancements could be concluded for this spectrum. There is no inconsistency with the balloon-borne measurements, since ozone above 37 km is only a fraction of the total ozone column observed from the ground. Subsequently, the two medium optical path scans from the June 6, 1988, flight were analyzed, mostly with the spectral least squares method. Figure 9 shows some of the narrow interval fits, with selected temperature insensitive isotopic lines. The resulting column-averaged enhancements ratios are 1.16 ± 0.08 and 1.25 ± 0.12 for $^{16}O^{18}O^{16}O$ and $^{16}O^{16}O^{18}O$, respectively. The error limits are smaller than obtained for the November 1987 flight spectra primarily because of improvements in the phase corrections of the spectra. Since the enhancements results for both balloon flights are insensitive to the assumed ozone vertical distribution, a reference ozone distribution was used in the present analysis [*Smith*, 1982]. Summary of the spectral lines used in the single lines analysis for both flights are shown in Table 1. The consistency between the two flights is satisfactory.

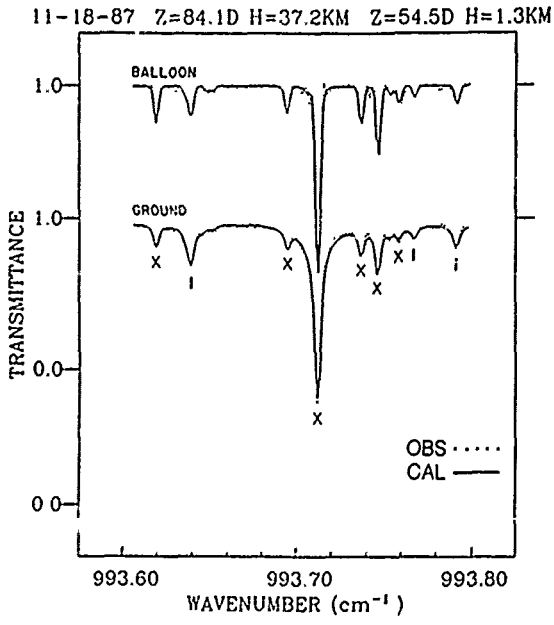

Fig. 8 Spectral least squares fitting of ground-based (bottom curves) and balloon-borne solar spectra (top curves) in the 993.60–993.80 cm^{-1} region. The spectra were obtained prior to and during a balloon flight on November 18, 1987, from Fort Sumner, New Mexico, with the University of Denver 0.002 cm^{-1} resolution interferometer.

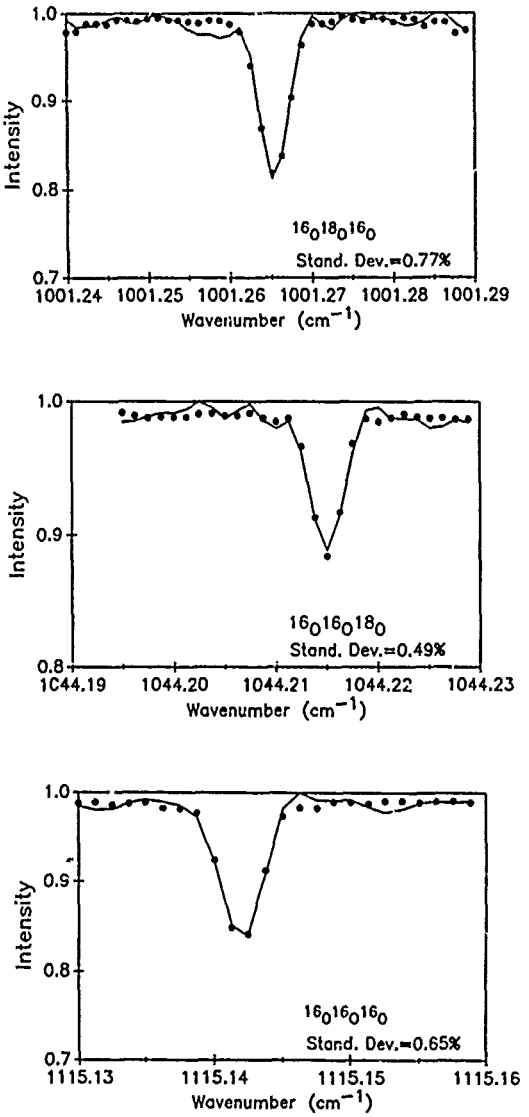

Fig. 9. Spectral least squares fittings of a balloon-borne solar spectrum obtained at an astronomical zenith angle of 87.31° during a balloon flight on June 6, 1988. The fit is for selected narrow intervals, dominated by isolated $^{16}O^{18}O^{16}O$, $^{16}O^{16}O^{18}O$, and $^{16}O^{16}O^{16}O$ isotopic lines. The measured spectrum is shown as a solid line; the least squares best fit spectrum is plotted with solid circles

Previous measurements have shown considerable variability in the enhancement of heavy ozone over a wide altitude range in the stratosphere. *Mauersberger* [1987] has measured altitude profiles of mass 50 ozone obtained from three balloon flights. The measurements do not discriminate between the asymmetric and symmetric forms of heavy ozone. The profiles show variable mass 50 enhancements at high altitude, with values of 15–20% at 37 km and 20–40% at 43 km, the upper latitude limit of the measurements [*Mauersberger*, 1987, Figure 2]. Our results fall within the range. The far-infrared measurements of *Abbas et al.* [1987] indicated

TABLE 1. Positions, Intensities, Air-Broadened Half Widths, Lower-State Energies, and Rotational Assignments for $^{16}O^{18}O^{16}O$ (=686), $^{16}O^{16}O^{18}O$ (=668), and $^{16}O_3$ (=666) Lines Used in Spectral Least Squares Fits to University of Denver Stratospheric Solar Absorption Spectra

Isotopic Species	Line Position, cm^{-1}	Intensity, 10^{-22} cm^{-1}/molecule cm^{-1} at 296 K	Width, cm^{-1} atm^{-1} at 296 K	Lower State Energy, cm^{-1}	Rotational Assignment					
					J'	K_a'	K_c'	J''	K_a''	K_c''
686	989.1117	0.520	0.0749	221.9696	19	4	15	20	4	16
	991.4716	0.660	0.0759	156.9273	17	2	15	18	2	16
	992.7679	0.680	0.0764	139.0045	16	2	15	17	2	16
	993.7910	0.461	0.0775	172.1693	14	5	10	15	5	11
	1001.2660	0.491	0.0818	41.7431	7	2	5	8	2	6
	1001.2680	0.534	0.0818	33.9264	7	1	6	8	1	7
668	1043.0710	0.597	0.0730	232.5346	25	0	25	24	0	24
	1043.3900	0.564	0.0725	251.8811	26	1	26	25	1	25
	1043.4400	0.589	0.0734	230.3679	24	2	23	23	2	22
	1043.4520	0.479	0.0734	268.9298	24	4	20	23	4	19
	1043.5310	0.637	0.0744	198.5708	22	2	20	21	2	19
	1043.6800	0.633	0.0739	208.0322	23	1	22	22	1	21
	1043.6870	0.540	0.0734	247.3170	24	3	22	23	3	21
	1043.7920	0.532	0.0721	271.6699	27	1	27	26	1	26
	1044.0130	0.455	0.0730	288.0557	25	4	21	24	4	20
	1044.0300	0.370	0.0725	335.4684	26	5	22	25	5	21
	1044.2170	0.512	0.0730	266.4059	25	3	23	24	3	22
666	1101.9460	1.25	0.0749	191.7092	21	1	21	20	2	18
	1115.1441	1.11	0.0730	269.2148	24	3	21	24	2	22
	1140.9448	1.02	0.0744	190.2125	22	2	20	21	1	21
	1146.4715	3.95	0.0713	372.4103	29	4	26	28	3	25
	1155.5132	2.84	0.0787	189.0092	14	7	7	13	6	8
	1163.4222	2.57	0.0775	253.8827	16	8	8	15	7	9
	1178.1545	1.05	0.0799	366.7466	12	11	1	11	10	2

Intensities are for natural abundance. Single and double primes denote upper and lower states, respectively. All 686 and 668 lines are transitions of the respective ν_3 fundamental bands. All 666 lines are transitions of the ν_1 fundamental band. The 1001.2660 and 1001.2680 cm^{-1} lines of 686 are unresolved in the solar spectra; all other lines appear as resolved features.

13–45% enhancement of mass 50 ozone between 25 and 37 km altitude, with $^{16}O^{18}O^{16}O$ preferentially enhanced relative to $^{16}O^{16}O^{18}O$ (except at 25 km). The present results show a smaller enhancement of mass 50 ozone (33% for the 1987 flight and 22% for the 1988 flight above 37 km, as compared to the 45% measured by *Abbas et al.* [1987] at 37 km). Although the error limits overlap, our enhancements are larger for the asymmetric form than for the symmetric form, which is opposite to the measurements of *Abbas et al.* [1987]. *Carli and Park* [1988] have analyzed far-infrared spectra recorded with the same instrument during an earlier balloon flight to obtain altitude profiles of mass 50 ozone. These results indicate an ~10% enhancement of total mass 50 ozone above 28 km (near the error limit of the experiment) with no detectable altitude dependence in the enhancement or difference between $^{16}O^{18}O^{16}O$ and $^{16}O^{16}O^{18}O$.

Experiments have also shown enhancements in mass 50 ozone produced by several methods in the laboratory (*Thiemens and Jackson* [1987], *Bhattacharya and Thiemens* [1988], and *Anderson et al.* [1989] and the references cited therein). The recent laboratory measurements of *Anderson et al.* [1989] are consistent with our balloon results of $^{16}O^{16}O^{18}O$ being enriched approximately twice as much as $^{16}O^{18}O^{16}O$. While most theoretical calculations [*Kaye and Strobel*, 1983; *Kaye*, 1986] predict negligibly small isotopic enhancement, it appears that the processes involved are not fully understood [*Bates*, 1988]. Some of these studies indicate that the enhancement should be in the $^{16}O^{16}O^{18}O$. The analysis reported in this paper has the high-resolution advantage for isolating isotopic O_3 lines and is based on the best currently available spectral line parameters. Further improvements of the accuracy of the measurements require higher signal to noise ratio and less spectral distortion of the data. We expect that future laboratory work will allow $^{16}O^{17}O^{16}O$ and $^{16}O^{16}O^{17}O$ lines to be identified in the balloon flight spectra, yielding important new quantitative information on the processes producing heavy ozone enhancement in the stratosphere.

We have also used a tunable diode laser heterodyne spectrometer to record extremely high resolution (0.0004 cm^{-1}) ground-based solar spectra in narrow intervals of the 9.6-μm ozone band [*McElroy et al.*, 1989]. The paper shows samples of these spectra with more resolved lines as well as spectral least squares O_3 quantifications. It is apparent that despite the pressure broadening of the lower stratosphere and upper troposphere O_3 lines, resolutions better than 0.002 cm^{-1} provide more complete information on the O_3 line shapes, which could be used in deriving vertical profile. Yet the balloon flight data analyzed here have the resolution necessary for accurate quantification of the column-averaged ^{18}O-isotopic ozone enhancement at high altitudes.

Acknowledgments. This research was supported in part by the National Aeronautics and Space Administration and in part by the National Science Foundation. Acknowledgment is made to the National Center for Atmospheric Research, which is supported by the National Science Foundation, for computer time used in this research.

REFERENCES

Abbas, M. M., J. Guo, B. Carli, F. Mencaraglia, M. Carlotti, and J. G. Nolt, Heavy ozone distribution in the stratosphere from far-infrared observations, *J. Geophys. Res.*, *92*, 13,231–13,239, 1987.

Anderson, S. M., J. Morton, and K. Mauersberger, Laboratory

measurements of ozone isotopomers by tunable diode laser absorption spectroscopy, *Chem. Phys. Lett.*, in press, 1989.
Bates, D. R., Suggested explanation of heavy ozone, *Geophys. Res. Lett.*, *15*, 13–16, 1988.
Bhattacharya, S. K., and M. H. Thiemens, Isotopic fractionation in ozone decomposition, *Geophys. Res. Lett.*, *15*, 9–12, 1988.
Camy-Peyret, C., J.-M. Flaud, A. Perrin, V. Malathy Devi, C. P. Rinsland, and M. A. H. Smith, The hybrid-type bands ν_1 and ν_3 of $^{16}O^{16}O^{18}O$: Line positions and intensities, *J. Mol. Spectrosc.*, *118*, 345–354, 1986.
Carli, B., and J. H. Park, Simultaneous measurement of minor stratospheric constituents with emission far-infrared spectroscopy, *J. Geophys. Res.*, *93*, 3851–3865, 1988.
Cicerone, R. J., and J. L. McCrumb, Dissociation of isotopically heavy O_2 as a source of atmospheric O_3, *Geophys. Res. Lett.*, *7*, 251–254, 1980.
Flaud, J.-M., C. Camy-Peyret, V. Malathy Devi, C. P. Rinsland, and M. A. H. Smith, The ν_1 and ν_3 bands of $^{16}O^{18}O^{16}O$: Line positions and intensities, *J. Mol. Spectrosc.*, *118*, 334–344, 1986.
Flaud, J.-M., C. Camy-Peyret, V. Malathy Devi, C. P. Rinsland, and M. A. H. Smith, The ν_1 and ν_3 bands of $^{16}O_3$: Line positions and intensities, *J. Mol. Spectrosc.*, *124*, 209–217, 1987.
Goldman, A., T. G. Kyle, D. G. Murcray, F. H. Murcray, and W. J. Williams, Long path atmospheric ozone absorption in the 9-10-μ region observed from a balloon-borne spectrometer, *Appl. Opt.*, *9*, 565–580, 1970.
Goldman, A., R. D. Blatherwick, F. J. Murcray, J. W. Van Allen, F. H. Murcray, and D. G. Murcray, New atlas of stratospheric IR absorption spectra, vol. I, Line positions and identifications; Vol. II, The spectra, NSF Scientific report, Dep. of Physics, Univ. of Denver, Colo., 1987.
Goldman, A., R. D. Blatherwick, F. J. Murcray, J. W. Van Allen, J. J. Kosters, F. H. Murcray, and D. G. Murcray, New atlas of high resolution infrared stratospheric spectra, NSF Scientific report, Dep. of Physics, Univ. of Denver, Colo., 1988.
Hartmann, J. M., C. Camy-Peyret, J.-M. Flaud, J. Bonamy, and D. Robert, New accurate calculations of ozone line-broadening by O_2 and N_2, *J. Quant. Spectrosc. Radiat. Transfer*, *40*, 489–495, 1988.
Kaye, J. A., Theoretical analysis of isotope effects on ozone formation in oxygen photochemistry, *J. Geophys. Res.*, *91*, 7865–7874, 1986.
Kaye, J. A., Mechanisms and observations for isotopic fractionation of molecular species in planetary atmospheres, *Rev. Geophys.*, *25*, 1609–1658, 1987.
Kaye, J. A., and D. F. Strobel, Enhancement of heavy ozone in the Earth's atmosphere, *J. Geophys. Res.*, *88*, 8447–8452, 1983.
Malathy Devi, V., J.-M. Flaud, C. Camy-Peyret, C. P. Rinsland, and M. A. H. Smith, Line positions and intensities for the $\nu_1 + \nu_2$ and $\nu_2 + \nu_3$ bands of $^{16}O_3$, *J. Mol. Spectrosc.*, *125*, 174–183, 1987.
Mauersberger, K., Measurements of heavy ozone in the stratosphere, *Geophys. Res. Lett.*, *8*, 935–937, 1981.
Mauersberger, K., Ozone isotope measurements in the stratosphere, *Geophys. Res. Lett.*, *14*, 80–83, 1987.
McElroy, C. T., A. Goldman, and D. G. Murcray, Heterodyne spectrophotometry of ozone in the 9.6 micron band using a tunable diode laser, *Appl. Opt.*, in press, 1989.
Pickett, H. M., E. A. Cohen, L. R. Brown, C. P. Rinsland, M. A. H. Smith, V. Malathy Devi, A. Goldman, A. Barbe, B. Carli, and M. Carlotti, The vibrational and rotational spectra of ozone for the (0, 1, 0) and (0, 2, 0) states, *J. Mol. Spectrosc.*, *128*, 151–171, 1988.
Rinsland, C. P., V. Malathy Devi, J.-M. Flaud, C. Camy-Peyret, M. A. H. Smith, and G. M. Stokes, Identification of ^{18}O-isotopic lines of ozone in infrared ground-based solar absorption spectra, *J. Geophys. Res.*, *90*, 10,719–10,725, 1985.
Rinsland, C. P., M. A. H. Smith, J.-M. Flaud, C. Camy-Peyret, and V. Malathy Devi, Line positions and intensities of the $2\nu_3$, $\nu_1 + \nu_3$, and $2\nu_1$ bands of $^{16}O_3$, *J. Mol. Spectrosc.*, *130*, 204–212, 1988.
Rothman, L. S., R. R. Gamache, A. Goldman, L. R. Brown, R. A. Toth, H. M. Pickett, R. L. Poynter, J.-M. Flaud, C. Camy-Peyret, A. Barbe, N. Husson, C. P. Rinsland, and M. A. H. Smith, The HITRAN database: 1986 edition, *Appl. Opt.*, *26*, 4058–4097, 1987.
Smith, M. A. H., Compilation of atmospheric gas concentration profiles from 0 to 50 km, *NASA Tech. Memo. 83289*, NASA Langley Research Center, Hampton, Va., 1982.
Smith, M. A. H., C. P. Rinsland, V. Malathy Devi, D. C. Benner, and K. B. Thakur, Measurements of air-broadened and nitrogen-broadened half-widths and shifts of ozone lines near 9 μm, *J. Opt. Soc. Am.*, *5*, 585–592, 1988.
Thiemans, M. H., and T. Jackson, Production of isotopically heavy ozone by ultraviolet light photolysis of O_2, *Geophys. Res. Lett.*, *14*, 624–627, 1987.

A. Barbe, Faculty of Sciences, Reims University, Reims 51062, France.
J.-M. Flaud and C. Camy-Peyret, Laboratory of Molecular and Atmospheric Physics, Pierre and Marie Curie University, Paris 75252, France.
A. Goldman, F. J. Murcray, D. G. Murcray, and J. J. Kosters, Department of Physics, University of Denver, Denver, CO 80208.
C. P. Rinsland, Atmospheric Sciences Division, NASA Langley Research Center, Hampton, VA 23665.

(Received November 30, 1988;
revised March 6, 1989;
accepted March 6, 1989.)